Examination of the High Load Limit of an HCCI Engine

by

Nathan Anderson

B.S., Mechanical Engineering
Michigan Technological University, 2006

SUBMITTED TO THE DEPARTMENT OF MECHANICAL ENGINEERING IN PARTIAL FULFULLMENT OF THE REQUIREMENTS FOR THE DEGREE OF

MASTER OF SCIENCE IN MECHANICAL ENGINEERING
AT THE
MASSACHUSETTS INSTITUTE OF TECHNOLOGY

February, 2008

Signature of Author: _____

Department of Mechanical Engineering
December 21, 2007

Certified by: _____

Wai K. Cheng
Professor of Mechanical Engineering
Thesis Supervisor

Accepted by: _____

Lallit Anand
Chairman, Departmental Graduate Committee

This page left intentionally blank.

Examination of the High Load Limit of an HCCI Engine

By

Nathan C. Anderson

Submitted to the Department of Mechanical Engineering on February 1, 2008
in partial fulfillment of the requirements for the Degree of Master of Science in
Mechanical Engineering

ABSTRACT

The implementation of homogenous charge compression ignition (HCCI) to gasoline engines is constrained by many factors. This work examines constrains imposed by nitric oxide (NO_x) emission and by the need to maintain a minimum catalyst temperature on HCCI operation. Then the nature of the approach to high load limit was examined for three fuels with very different behavior.

An engine simulation was used to examine constrains imposed by NO_x emission and by catalyst temperature requirement. The valve timing in a HCCI engine using Negative-Valve-Overlap (NVO) was varied in the simulation to control the operating point. The engine speed and intake pressure (turbocharged mode) were varied. The High Load Limit (HLL) was attained when the NO_x emission reached the regulated level for a Partial-Zero-Emissions-Vehicle (PZEV). This occurred when the engine was running at the lowest speed and the highest intake pressure. Unreasonably large residual fraction was required to achieve the NO_x limit unless a three-way catalyst is used.

The engine behavior in the operating trajectory to the HLL was examined by using two Primary Reference fuels (PRF60 and PRF90) and a fuel blended from refinery feed stock. The latter fuel had Extremely Low Aromatic and Olefin content and is referred to as the ELAO fuel. For PRF60 (the knock prone fuel), the Maximum Pressure Rise Rate (MPRR) increased with increase in load (by reduction of residual). The HLL was attained when the MPRR reached a pre-determined level of 5MPa/ms. For PRF90 (the knock resistant fuel), however, the MPRR decreased with increase in load, and the HLL was constrained by ignition failure. For the ELAO fuel, the MPRR first increased and then decreased with increase in load. The HLL was thus constrained by ignition failure. Thus depending on the fuel properties, there could be very different engine behaviors in the approach to the HLL of HCCI operation.

Thesis Supervisor: Wai K. Cheng
Title: Professor of Mechanical Engineering

Table of Contents

Table of Equations, Figures, and Tables

1 Introduction

1.1 **Background**:

Homogenous charge compression ignition (HCCI), or as it is sometimes referred to, controlled auto-ignition (CAI), is the compression-ignition of a premixed charge inside of an internal combustion engine. HCCI is the combination of principles commonly associated with spark ignition (SI) and compression ignition (CI) engines. The homogenous charge is used in SI engines where a pre-mixed (homogenous) charge is inducted into the cylinder and that mixture is then ignited using a spark. Inside of a CI engine, only fresh air is brought into the cylinder and then fuel is directly injected into the hot compressed air when the piston is near its top position. The fuel injected initially mixes with the hot air and auto-ignites; then the subsequently injected fuel is sprayed into the hot charge and burns as a diffusion flame.

HCCI combines those two ideas and creates a third combustion system. The main difference between the three systems is the control of the combustion. In both SI and CI engines, there is an event which triggers the combustion (spark timing in SI and injection timing in CI). Such a definitive triggering event is lacking in HCCI, which is controlled by combustion chemical kinetics and the charge thermal environment.

HCCI was described in 1979 by Onishi at the Nippon Clean Engine Research Institute [1]. He developed a method to take the auto-ignition that was a common abnormal combustion in a two stroke engine and developed it into a consistent mode of engine operation that allowed for greater lean operation. The normally high residual

fractions associated with the two-stroke engine is what allowed for, what he referred to as, Active Thermo-Atmosphere Combustion (ATAC) to occur. The hot residual gases had provided sufficient trapped energy that when the mixture temperature was further increased due to compression, the mixture would auto-ignite.

After this initial work on two stroke engines it was four years later until this new combustion system was achieved in a four-stroke engine by Najit and Foster [2]. Once the combustion system was implemented into a four-stroke engine a wide range of possibilities became available. There are two main paths that the HCCI research can be taken and those two paths are based upon the origins of the combustion itself. A HCCI engine can be either based upon a CI (diesel) or SI (gasoline) engine. The largest difference is in the way the auto-ignition is achieved. With CI based HCCI, a high compression ratio is used bring the mixture to auto-ignition. SI based HCCI, on the other hand, requires an additional source of enthalpy to make up for the lower temperature rise due to the lower compression ratio. Initially, testing was done with increased increase intake air temperatures, but increasingly the practice is to use trapped hot residual gasses instead to create the auto-ignition [3]. The process they used to trap the gasses is what is currently referred to as negative valve overlap (NVO). This means that exhaust-valve-close (EVC) happens substantially earlier than the intake-valve-open (IVO). The early EVC enables a large amount of hot residual fraction to be trapped.

Another issue which arises from the CI and SI basis is which type of fuel to use inside of an engine which has properties of both combustion systems. This is an issue of more importance for HCCI than it is for SI and CI based engines. This is because the combustion is controlled by chemical kinetics, so not only does the cylinder's thermal

performance come into question, but also the chemical make-up and behaviors of the fuels [4]. Some of the work of the most importance to this research is from Shibata and Urushihara [5] and also from Yao et. al. [6]. Yao et. al. showed that by using a wide difference of octane numbers in primary reference fuels (PRF) that there exists and optimal octane rating for a given operating condition and that higher octane fuels lend themselves to higher IMEP and lower octane fuels lend themselves to lower IMEP for a given operating condition [6]. This leads to the notion that for a given operating condition an ideal octane rating exists. Shibata and Urushiara however found that with increased intake air temperatures (50°C - 180°C) several effects presented themselves. First, is that with increased intake air temperature the start of combustion was advanced and low temperature heat release (LTHR) was removed. Also, as the intake temperature is increased, the differences between the start of the high temperature heat release (HTHR) is decreased between different fuels. It was concluded that increased intake air temperature is an effective way to reduce the differences caused by fuel chemistry. This has great implications toward the research previously conducted by M. Andrea [7] with this project's setup. It was shown that at the high load limit (HLL) that over a wide range of fuels (representative of the variation in the North American market) that fuel composition had little effect on the highest load achievable. Since this research uses NVO to trap hot residual gases, the temperature of the mixture at the start of compression will be of a much greater temperature than that of the inducted charge, which may reduce the performance differences in the fuels.

1.2 Motivation:

As described above, from the very beginning HCCI has always been looked towards with great expectations. Onishi looked towards this new combustion system in hopes of allowing lean two-stroke operation to not only reduce emissions, but to also reduce fuel consumption. The same hope still applies today in the application of HCCI in four-stroke engines. It shows the greatest promise in the improving upon SI engine performance allowing for both increased efficiency and decreased emissions. Since HCCI can be operated without a throttle it promises large gains in the mid-load "cruising" style applications, and because HCCI needs larger amounts of hot residual dilution to operate, this extra mass lowers the cycle temperature and thus reduces NO_x emissions.

While it does possess these great capabilities, it is not without significant drawbacks. As just mentioned, it really only functions well in a mid-load application, which fits within a very small operating range that does not include typical low and high loads that are present in a SI engine's operating range. This means that the benefits of running an HCCI engine cannot be passed onto idle conditions where increased efficiency could be very beneficial. Also, it does not posses a direct means of combustion control like SI or CI engines. This makes controlling the combustion events very difficult and possibly unreliable. It is these challenges which drive research forward. This research hopes to look at the HLL and the real world application limits to better understand what the limitations are.

1.3 Project Goals:

The research conducted by M. Andrea [7] may have concluded that no large variations are present at the HLL from the fuels representative of the N.A. market, but is there a spread of fuel properties that does show a difference? The answer to this question would simply provide a better glimpse of the governing factors that actually control the high load limit. It is not simply good enough to stop and say that the market fuels do not have show a difference it must be understood why they do not. It is the hope of this project to examine fuels with very different auto-ignition characteristics and to see how their performance varies at the HLL. Also, using simulation software [8] it is desired to find the LLL and HLL associated with real world limitations such as NO_x emissions regulations and catalyst light-off temperature.

1) Simulate NO_x emissions and Catalyst light-off temperature
2) Examine the performance of PRF90 and PRF60 at the HLL

1.4 Experimental Setup:

The engine used in the experiments and which the simulations were modeled was the same engine was used with previous experiments [7], [11]. The engine was a 2003 Mazda L3 2.3L inline 4-cylinder engine with the geometries as defined in table 1.1. The engine has been modified so that only one of the four cylinders fires. The only geometric modification that has been done to the engine block is that the piston of the firing cylinder has been modified so that a slightly higher compression ratio could be achieved.

Part	Dimension
Intake Runner	
Length	25 (mm)
Diameter	35 (mm)
Exhaust Runner	
Length	25 (mm)
Diameter	30 → 40 (mm)
Engine Block	
Bore	87.5 (mm)
Stroke	94 (mm)
Compression Ratio	11.1
Con. Rod.	154.8 (mm)
Wrist Pin Offset	0.8 (mm)
Clearance Height	10 (mm)

Table 1.1: Physical Engine Dimensions

The valve train is the most important, and most modified from the stock component of the engine for the HCCI engine. HCCI combustion was achieved with this engine by utilizing the negative valve overlap (NVO) scheme. This process actually pushes the exhaust valve close event and intake valve open even away from top center of the exhaust stroke (see figure 1.1). This allows for the residuals from the cycle's combustion to be trapped inside the cylinder instead of being pushed out of the exhaust. These hot gasses are the reason that the cold incoming charge is able to be auto-ignited. Control over the engine's load is achieved through the variable valve timing (VVT) on both the intake and exhaust camshafts. Initially, the stock engine only had VVT on the intake cam, but an additional cam-phaser was added to the exhaust camshaft. Each cam-phaser has the ability to shift the valve timings over a range of 35 CAD. This shifting ability and the requirements of HCCI combustion demanded that the camshafts be modified from their stock design. The new cams were designed such that the maximum flexibility and performance could be achieved with using the VVT. It was determined that a camshaft with 120 CAD valve opening duration would allow for the maximum operation range that was desired while still trapping enough residuals to maintain HCCI.

With the shortened valve opening duration, the valve lift has to be decreased to limit the cam stress. Both the intake and exhaust valves have a 2mm lift [7].

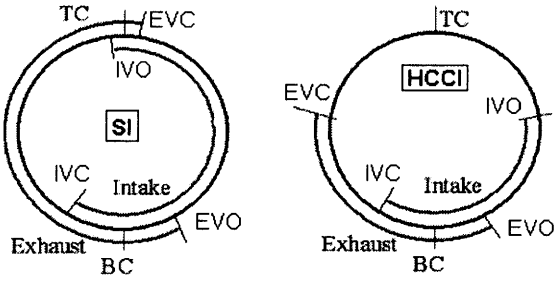

Figure 1.1: Comparison of SI (left) and HCCI (engine) valve timings. The HCCI valve timing represented is symmetric NVO timing.

2 HLL and LLL Simulations:

2.1 Model Setup:

A cycle simulation software (Ricardo WAVE) was utilized to develop a HCCI model which utilized the experimental engine's characteristics while allowing the analysis to examine the use of four cylinders instead of a single firing cylinder that the experimental uses. Figure 2.1 shows the model used, which was derived from a provided engine simulation in WAVE [8]. This simulation was used to approximate the combustion and the thermal fluid effects of gases through the engine. This model however does not do a detailed chemistry analysis of the combustion. The combustion is modeled by a simple Wiebe function, shown in figure 2.4 which is an idealized burn profile and is described further in section 2.3.

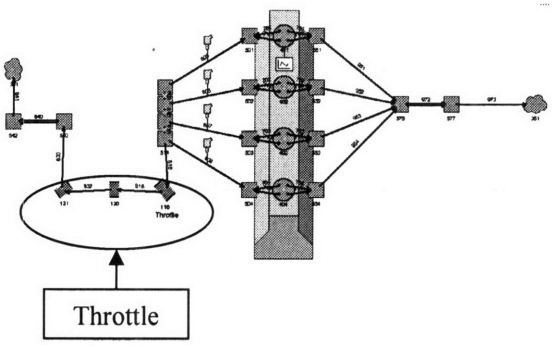

Figure 2.1: Original WAVE Model

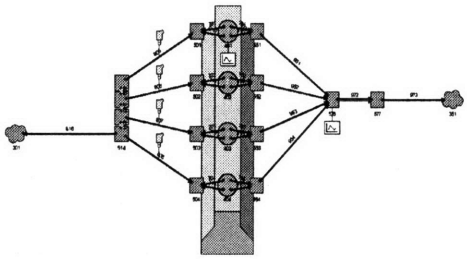

Figure 2.2: Modified WAVE Model (Throttle and piping removed)

2.2 Model vs. Physical Engine:

As is common with Research engines only a single cylinder is fired for a variety of reasons. Whether it is for limiting instrumentation complexity and cost or to limit the multi-cylinder effects on measurements such as lambda or emissions, single firing cylinder operation in a multi-cylinder engine is a very effective research practice but it is not without limitations. These limitations lead to the use of the 4-cylinder model instead of the single cylinder setup used by previous researchers [11]. The real world limits investigated by these simulations are affected in different ways and must be considered. Starting with the air intake, the inclusion of a plenum (which is not present in the experimental engine) supplied a large volume of air to the simulation and helped remove some inconsistencies that arose in early single cylinder results. These phenomena will be reviewed later, but without a plenum the acoustics (pressure waves) of the intake and exhaust air flow can have a significant effect [9] on the results of the simulations. The large volume of air stored in the plenum helps to control the variations in the air flow due to these acoustics.

The engine block's thermal characteristics were kept identical to the properties assigned by Ricardo [8] because the research engine's heat transfer coefficients would be very hard to measure accurately. When examining the NO_x production of the engine the burned gas temperature is one of the most important variables [10]. The load dependence of the NO_x emission is shown in Fig 2.3.

The catalyst is probably the most important addition to this model. Even though WAVE does not include a detailed chemistry model it is however capable of the thermal analysis required to predict the temperature of the catalyst. The catalyst is actually a collection of 5200 tubes each 0.2 cm in diameter and 11.8 cm long. The catalyst was one

of the main reasons behind implementing the multi-cylinder model. It would have been inaccurate to predict the catalyst temperature by simply using a single cylinder model. This is because given the 4-stroke IC engine cycle there would not be a constant flow of hot exhaust gasses leading to cooling that would not be present in a 4-cylinder model. With four cylinders running there is always one on the exhaust stroke so the catalyst is always exposed to a hot exhaust stream causing the catalyst to reach a greater temperature for a given set of conditions.

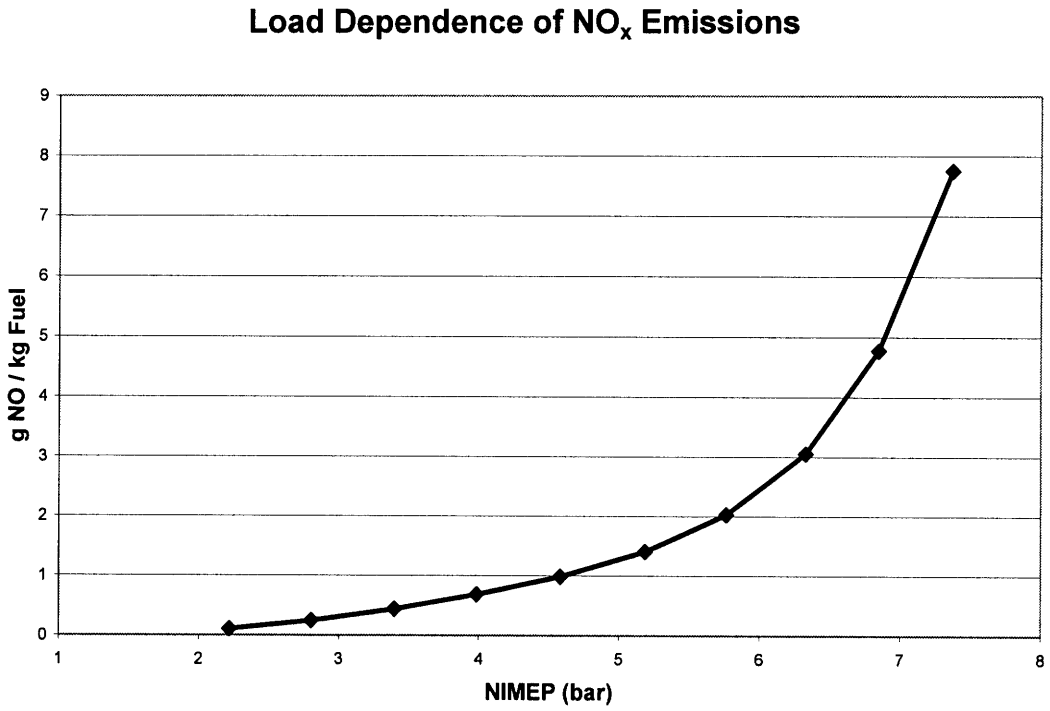

Figure 2.3: Increase in NO_x Production with load increase

2.3 Combustion:

The highlight of any HCCI project is the combustion process. While it is a combination of two very well documented processes (SI and CI) it is unique no the less. The main difference is the lack of a definite ignition source. With SI there is the spark, with CI there is the injection point, but with HCCI the start of combustion is controlled

by the fuel's chemistry. The start of combustion can be modeled with some basic fuels, such as PRF 90, but these are very detailed chemical simulations far too detailed for these simulations. A Wiebe function is used to model the heat release process. The Wiebe function (figure 2.4) is a simple s-function to model the mass fraction burned as a function of crank angle [9]. To model the HCCI combustion the combustion duration is shorter (compared to a typical SI value) and the 50% mass fraction burned was relocated. Typical SI combustion can have a 10-90% burn duration of approximately 30 CAD [9], but since HCCI is ideally instantaneous the 10-90 burn duration is much shorter at approximately 10 CAD. In this model this value is set to be constant along with the other defining parameter the location of 50% mass fraction burned (CAD50). Holding these two parameters (burn duration and CAD50) constant throughout the different operating points is another approximation. Combustion is very heavily dependent upon the initial conditions inside of the cylinder and multiple other variables. These initial conditions can vary cycle to cycle, with engine speed, intake pressure, and various other parameters. The combustion's CAD50 can change along with its burn duration depending upon all of these parameters. An additional simulation was done to examine the impact of varying both the burn duration and combustion phasing.

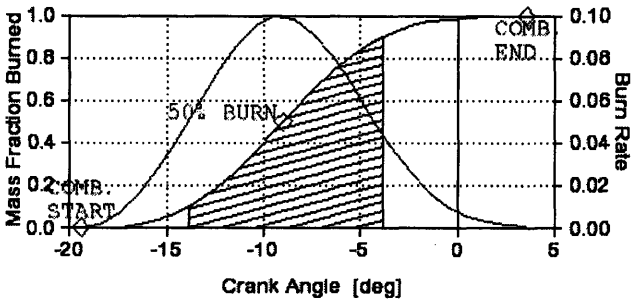

Figure 2.4: Wiebe Function

2.4 Simulation Setup:

HCCI combustion was achieved in the experimental engine by trapping hot residuals to increase the trapped enthalpy at intake valve closes so that auto-ignition was possible at the piston's top position (top dead center). This was achieved through a process called negative valve overlap (NVO). In this process the exhaust valve closes prior to top dead center (TDC) and the intake valve opens after TDC which results in a secondary compression / expansion cycle (figure 2.5). The type of NVO used in the experiments and in the simulations is called symmetric NVO (figure 1.1). This means that the exhaust valve closes and the intake valve opens the same CAD away from TDC. This minimizes the affect of the secondary compression so that there is not a pumping loop introduced into the cycle. This allows a truly non-throttled operation of the HCCI which is an efficiency gain over typical SI engines. The variable valve timing on the engine provides the necessary control to trap the desired amount of residuals inside the cylinder. Using the process of NVO the intake valve close and exhaust valve open were held constant while the other two events were varied with changing valve open duration while maintaining symmetry about TDC. The residual fraction controlled the amount of dilution the charge had, and also controlled the amount fresh charge which could be inducted. This process is slightly different than what is used by the experimental engine. The experimental engine has fixed cams and moves the location of both opening and closing events with a fixed valve open duration. Using the variable valve opening

duration allows for a greater control of the residual fraction and easier to discern the effects of the changing residual fraction.

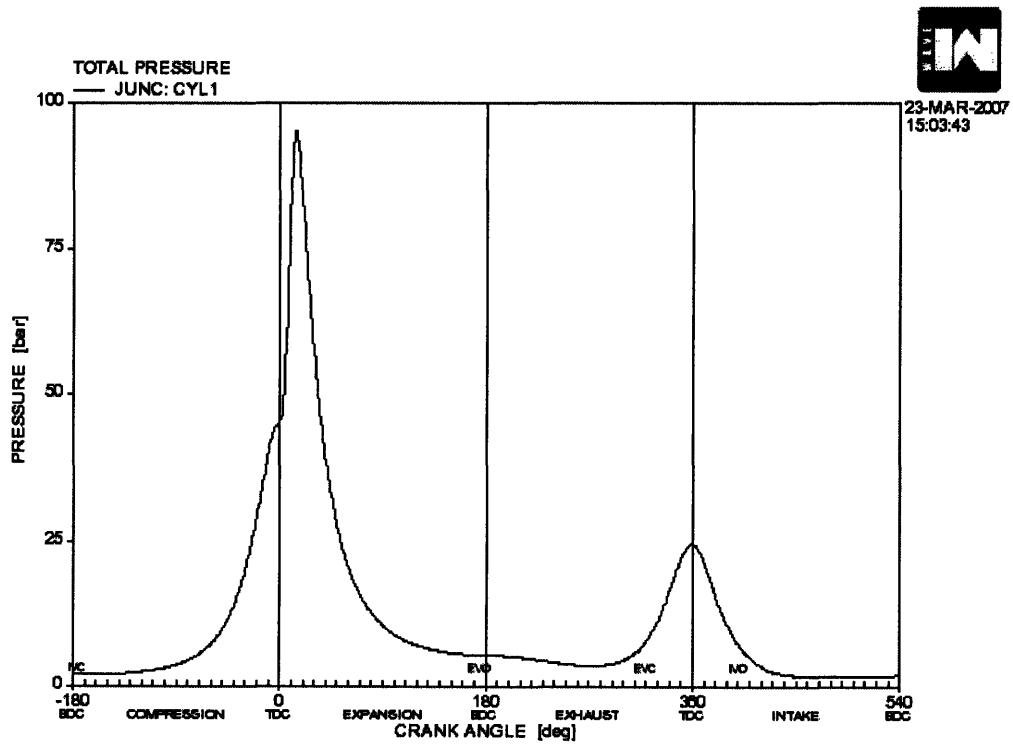

Figure 2.5: Pressure trace of HCCI combustion with symmetric NVO timing

Increasing the intake pressure (commonly referred to as boosting) of the simulation allowed for an examination of the effects of increased intake pressure on the engine. The simulation however did not model any boosting machinery (turbochargers, superchargers, etc.). The increased intake pressure was achieved by changing the ambient conditions in the model. This was done so that the model did not include the complicated analysis required for turbochargers / superchargers. The temperature was held also constant and only the pressure was varied. This is similar to the turbocharge / intercool configuration. Simplifying the simulation in this way removed any unnecessary variables associated with the turbo-machinery and allowed for the analysis to only include the effects of the increased intake density.

2.5 Simulation Process:

The effects of three parameters on the High Load Limit (HLL) and the Low Load Limit (LLL) were investigated. Those parameters were the engine speed, intake pressure, and residual fraction. The engine speed and intake pressure were held constant for a particular simulation run, while the valve timing were varied such that the residual fraction was varied from approximately 35% to 75%. This provided an approximation of the span of residual fractions that can be achieved inside of an HCCI engine. These limits however are exactly what is being studied in the experimental engine and the exact residual fraction at those limits is still undetermined as there is not exact way to measure the residual fraction inside an engine. Once each run was completed over the desired residual fraction range, the speed or intake pressure was changed (only one at a time however) and then the valve timings were swept again to achieve the desired residual fractions. This was done in 500 RPM increments from 1000RPM to 3000RPM and in 0.5 bar increments from 1 (atmospheric) to 3 bar.

2.6 Definition of the Limits:

Both the HLL and the LLL were defined around real world goals. In the experimental portion the main focus was on the maximum output possible using a particular engine. The focus of the simulations was to predict what would be the maximum possible output of this type of combustion when constrained by real world of

emissions limits. The HLL was defined as a maximum allowable tailpipe out emission of 0.13 g NO_x / kg Fuel (PRF90) based upon the 0.015 g NO_x / mile tailpipe out requirement and a fuel economy of 24.5 mpg. One of the main goals of HCCI is to be able to run the engine without a NO_x catalyst for cost savings benefits. However, if these types of engines cannot reach emissions requirements without a catalyst one would obviously have to be outfitted. This would mean that the exhaust gasses must be hot enough to allow the catalyst to reach its light-off temperature to be the most efficient. The catalysts light-off temperature is defined as the temperature at which the catalyst is greater than 50% efficient [9]. This is a possible issue with HCCI because its combustion occurs at a lower temperature which allows it to achieve the low NO_x emissions in the first place. The lowest load possible for operation would occur when the catalyst light off temperature of 600K is achieved and is thus defined as the low load limit.

2.7 HLL:

As mentioned above, the HLL is determined by a maximum NO_x emission. Nitric oxide is formed in the burned gas region of the charge because of the high temperatures. The simulation uses the burned gas temperature in the extended Zeldovich Mechanism (Figure 2.6) to calculate the NO_x emissions for that cycle. The analytical expressions are shown in Fig 2.7.

a) $N+NO \leftrightarrow N_2+O$

b) $N+O_2 \leftrightarrow NO+O$

c) $N+OH \leftrightarrow NO+H$

Figure 2.6: Extended Zeldovich Mechanism

$$R_a = A*ARC\ 1 \cdot e^{\left(\frac{T_a*AERC\ 1}{T}\right)}$$

$$R_{b,c} = A \cdot e^{\left(\frac{T_a}{T}\right)}$$

Figure 2.8: Arrhenius Equations for NOx Formation

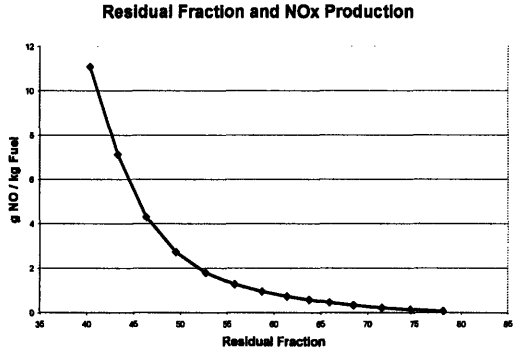

Figure 2.7: Exponential Relationship of NOx Production to Residual Fraction

$$T_b - T_u \propto \frac{1}{C_v}\left(\frac{(1-X_r)}{(1+A/F)}LHV - \frac{Q_L}{m_{TOT}}\right)$$

Figure 2.9: Burnt Gas Temperature Equation

The most important point to notice about these equations is the relationship to the residual faction. Looking at Figure 2.8 an exponential relationship clearly exists between the residual fraction and the NO_x production. This exists because of the equations in Figures 2.6 and 2.7. The Arrhenius equations are based upon an exponential formation equation with the burned gas temperature (T) in the denominator. The increasing burned gas temperature increases the rate constant because of the negative activation temperature (T_a). The burned gas temperature (Figure 2.9) is then controlled by the trapped charge and its composition (A/F, X_r, m_{TOT}, and C_v) and the heat losses during combustion (Q_L). This relationship is derived using a first law analysis of the system with the interior walls

of the combustion chamber as the control volume. Since this simulation is run using stoichiometric air-fuel ratio (A/F is constant) and at a constant speed and intake pressure holding heat transfer close to constant, increasing the residual fraction will thus decrease the burned gas temperature. This relationship is close to linear, but the linear change in temperature will cause an exponential change in the NO_x production.

2.7.1 Effects of Engine Speed:

Engine speed is an important component to vehicle operation. To examine HCCI limits it is necessary to vary the engine's speed to see what effect it will have on the NO_x production. Holding intake pressure constant, and sweeping through the range of residual fractions, the speed is then varied for each residual fraction sweep from 1000RPM to 3000RPM. These speeds are typical of the experimental engine's operating range. The speeds are stepped in 500RPM increments and the results for constant pressure of 1.0 bar of intake pressure are shown in Figure 2.10.

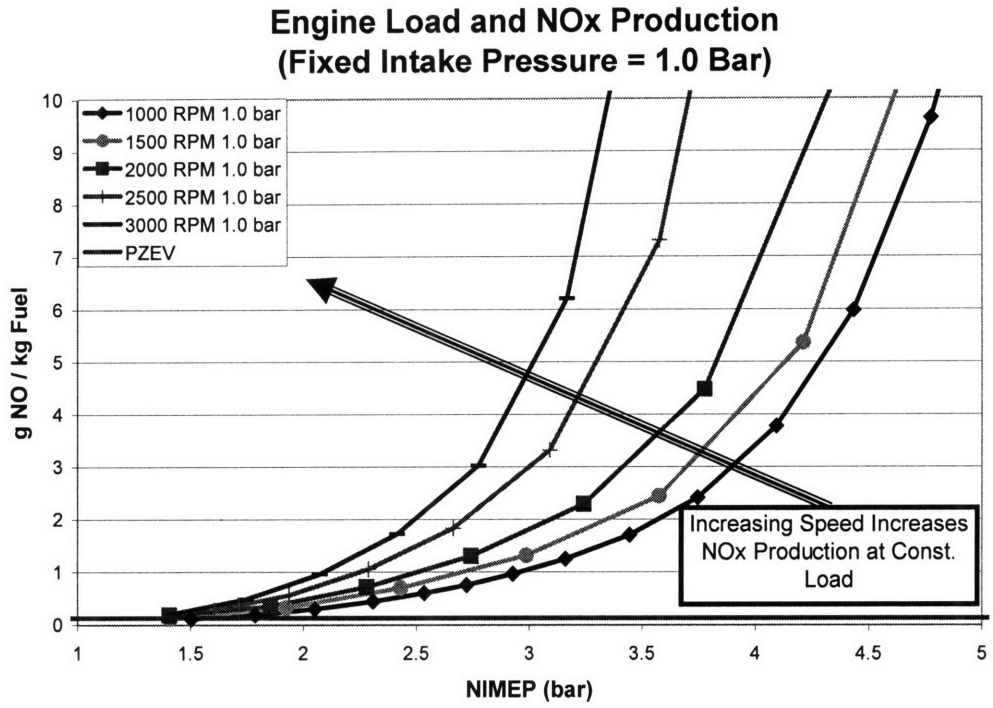

Figure 2.10: NOx Production and NIMEP at Various Speeds (1000-3000RPM)

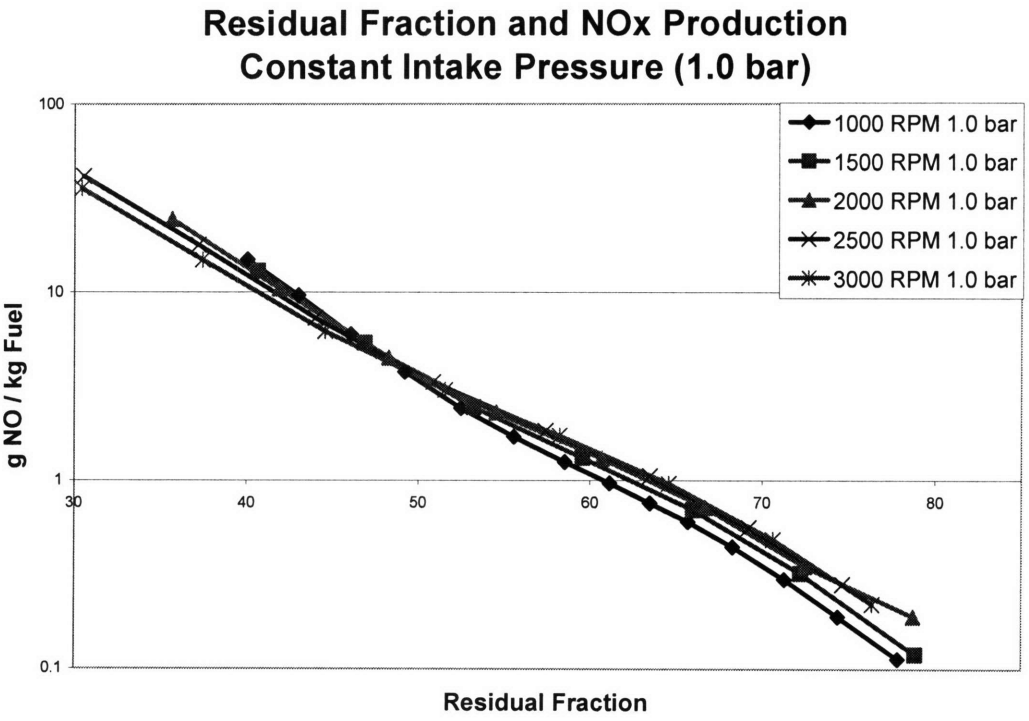

Figure 2.11: Log NOx Production and Residual Fraction at Various Speeds

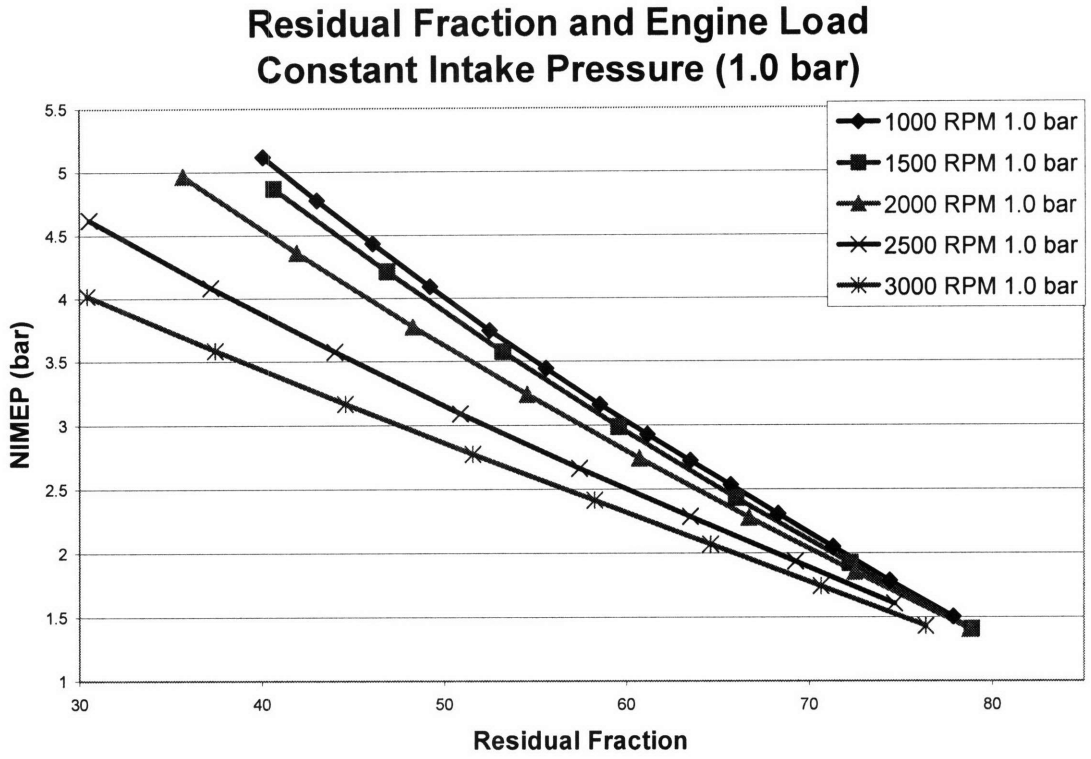

Figure 2.12: NIMEP and Residual Fraction at Various Speeds (1000-3000RPM)

The lines on Figure 2.10 show the NIMEP and the g NO / kg Fuel for a constant speed and constant intake pressure. The red horizontal line represents the PZEV tailpipe out emissions (0.13 g NO / kg fuel) which was used as the metric for determining the high load limit. This figure shows that as the engine speed increases there is also an increase in the NO_x production at a constant load. Figure 2.10 is actually the combination of Figures 2.11 and 2.12. As shown in Figure 2.9 the burnt gas temperature is determined by several factors, one of which is the residual fraction. Figure 2.11 shows that over the wide range of speeds, the specific NO production is only a function of residual gas fraction. Thus the main driving point force for the difference in NO production as a function of NIMEP is given by Figure 2.12. With increasing speed the engines load decreases at a given residual fraction. This is due to the decrease in the air

ingested, hence the fuel burned, as the A/F is kept stoichiometric. As the engines speed increases the amount of air that is able to be delivered decreases due to the air flow losses in the intake system. The measure of the intake's ability to deliver air to the cylinder is called the volumetric efficiency and, as shown in Heywood's text [9], the volumetric efficiency decreases with increasing engine speed. This effect also scales with square of the air flow which is determined by the engine speed, so ignoring the effects of intake tuning, this square factor becomes dominant in reference to the NO_x production and engine load. So, while NO_x production at a given residual fraction is approximately constant, the NIMEP at the same residual fraction varies greatly with speed and leads to Figure 2.10 with increasing speed causing decreased load for a given NO_x production.

2.7.2 Effects of Intake Pressure:

A common practice in modern engines is to downsize the engine size while increasing the intake pressure to induct more fuel into the system to get more power from the same volume. Changing the mass of the system has an impact on the production of NO_x as noted before and Figure 2.13 shows the results of holding the intake speed constant (1000rpm, and then sweeping through the desired residual fractions for each intake pressure ranging from 1.0bar to 3.0bar in 0.5 bar increments.

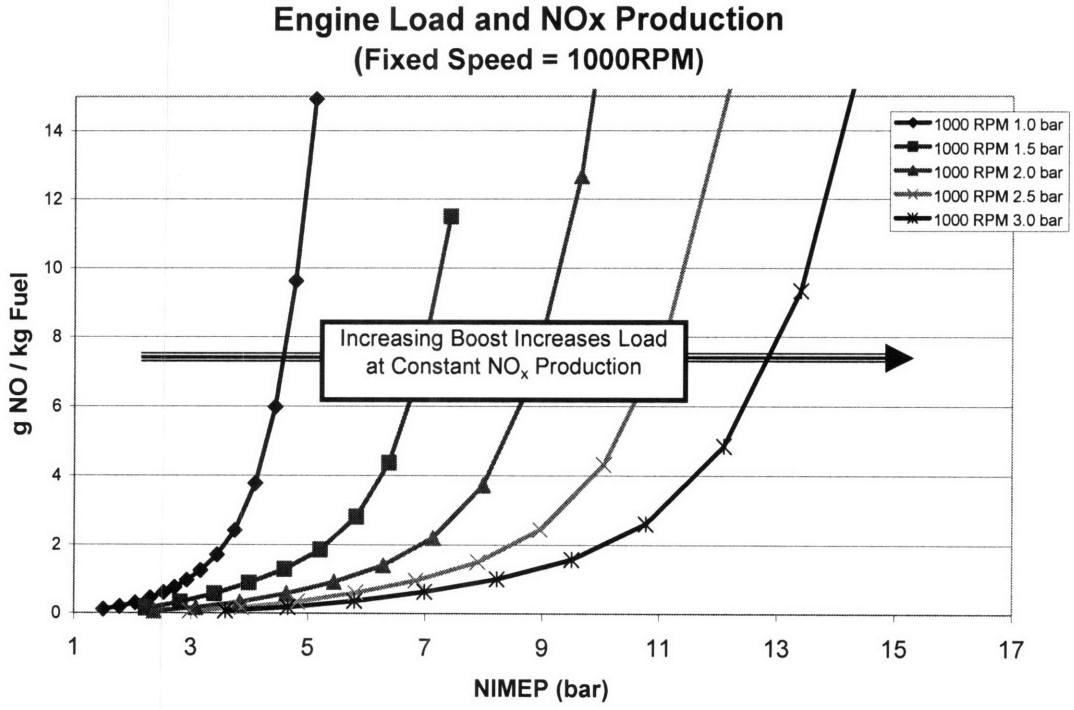

Figure 2.13: NIMEP and NOx Production at Various Intake Pressures (1 – 3 bars)

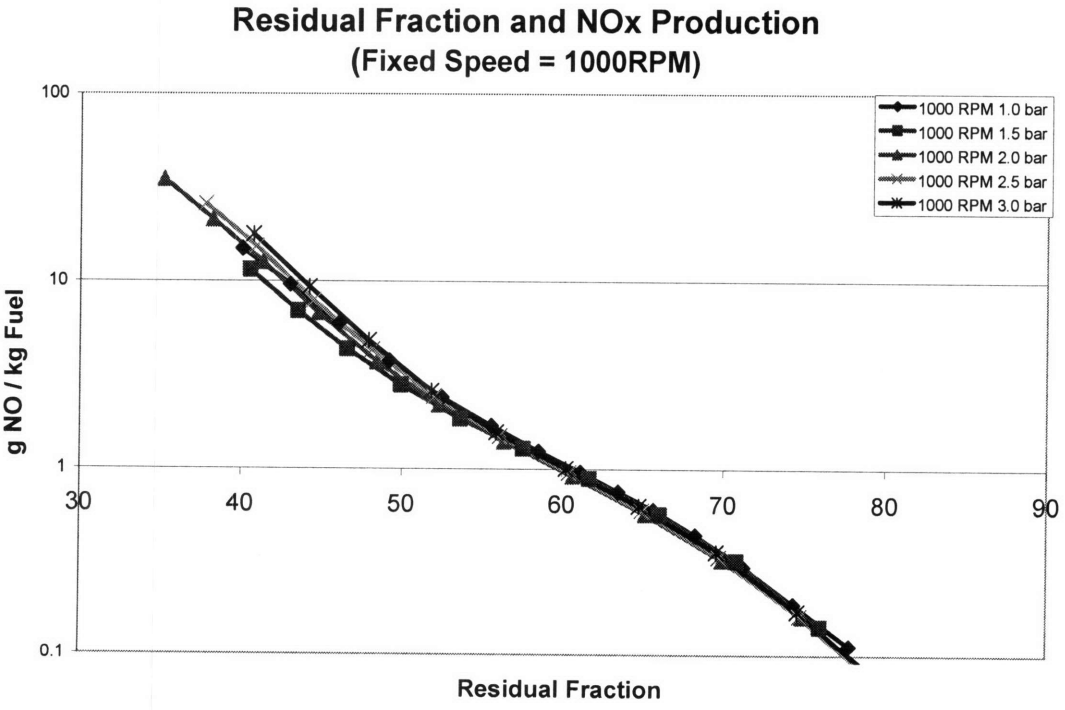

Figure 2.14: Residual Fraction and NOx Production at Various Intake Pressures

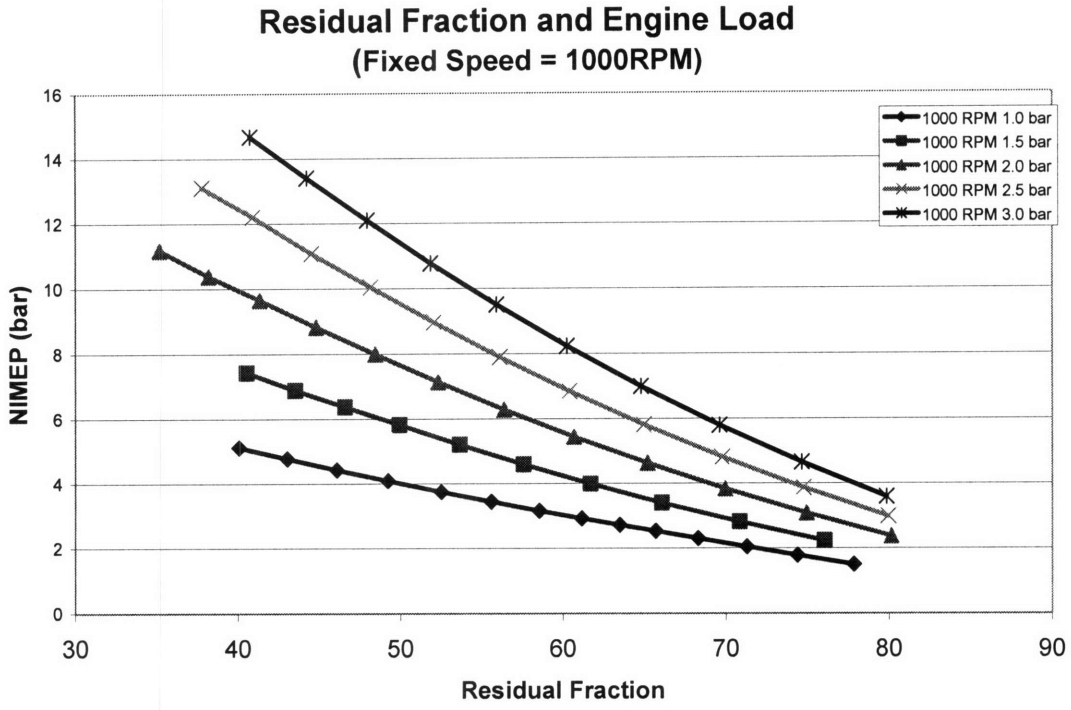

Figure 2.15: Residual Fraction and Engine Load at Various Intake Pressures

As described above for variations of engine speed, Figure 2.13 is a combination of Figures 2.14 and 2.15. Figure 2.14 shows the NO_x production in terms of residual fraction. As before with the varying speeds, there are variations between the different intake pressures, but on a larger scale they are approximately the same. Also, they do not follow a specific pattern which means there is no one dominant factor determining the relationship between NO_x production and varying intake pressures. As before the main dominating factor is the relationship between the residual fraction and the NIMEP. Approximating the NO_x production as constant for a given residual fraction and then looking at Figure 2.15 it is clear that this plot is determining the relationship of NO_x and engine load. The greater the intake pressure the denser the incoming air is, therefore, with a constant air-fuel ratio, this means more fuel (hence greater load) is also delivered

to the cylinder. This all leads to Figure 2.13 which shows that for a constant NO_x production increasing the boost pressure increases the load at that production rate. This also means for a given engine load increasing boost decreases the NO_x production at that load.

2.7.3 Load at the NO_x Production Limit:

As described above the High Load Limit is defined at the point at which the NO_x production reaches 0.13 g NO/kg Fuel. It was also shown that by decreasing the speed and also by increasing the intake pressure you can increase the engine load at a given NO_x production. This leads to the maximum load achievable by this simulation to occur when the engine is operating at 1000RPM with an intake pressure of 3.0 bars, at this operating condition the load at the HLL is 4.2 bar. Figure 2.16 shows 3 different speeds (1000, 2000, 3000 RPM) and 2 different intake pressures (1.0 and 3.0 bar) to illustrate how the engine behaves at the HLL. The largest increase in the engine load at the limit comes from the increase of the intake pressure (~2.7 bar increase in NIMEP), the lower speeds also contribute just in a smaller amount (~0.5 bar increase). This figure also illustrates how difficult it is to actually achieve this limit. These points require large amounts of dilution (>70% residual fraction) and some operating conditions do not even reach below the limit (2000 and 3000 rpm at 1.0 bar intake pressure). This leads to the point that the operation of an HCCI engine without a catalyst is very unlikely.

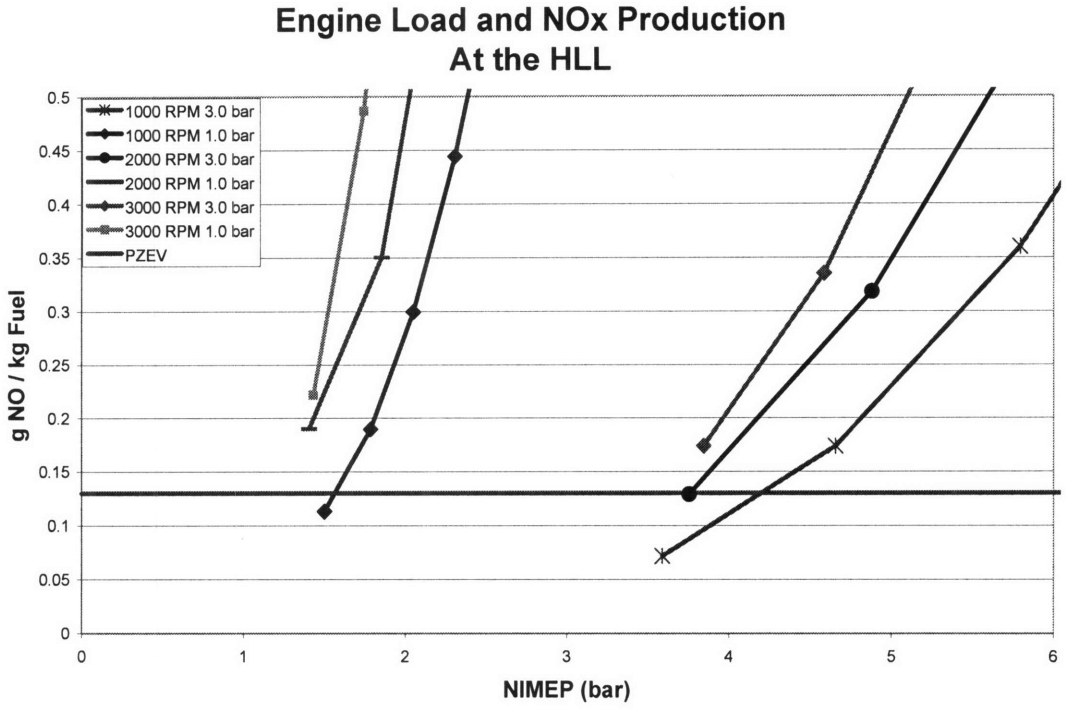

Figure 2.16: Engine Load and NOx Production at the High Load Limit

2.8 Low Load Limit (LLL) Required by Catalyst Light-Off:

The constraint of the LLL is the lowest load achievable at which the catalyst can achieve its light-off temperature. Usually this temperature is around 250 – 300 °C, so it was chosen that a light of temperature of 600K was to be used to be a little on the conservative side [9]. Since, it was very hard to get the engine to operate naturally below 0.13 g NO/kg Fuel, a catalytic converter must be used to allow for increased engine out NO_x emissions for a greater range of operation. This raises the question of whether or not the HCCI engine would produce enough hot exhaust gasses to raise the temperature of the catalyst to an acceptable operating temperature. In the same pattern as the HLL the

LLL was examined at multiple engine speeds (1000 – 3000 RPM) and intake pressures (1.0 – 3.0 bars).

2.8.1 Effects of Engine Speed:

The catalyst temperature T_{Cat} is obtained from a simple lump parameter model shown in Fig. 2.17. The catalyst inlet condition is calculated by the WAVE software using the engine operating condition and the heat loss in the exhaust runner. The exhaust gas temperature within the catalyst (T_{exh}) is the average of the inlet and outlet temperatures; the latter is determined by the overall heat balance. The steady state heat loss to the ambient air is given by $(hA)_{Exh.-Cat.}(T_{Ex.Gas} - T_{Cat.}) = (hA)_{Cat.-Amb}(T_{Cat.} - T_{Amb.})$. Thus the catalyst temperature may be solved by combining the above equation with the overall heat balance $\dot{m}(h_{in} - h_{out}) = (hA)_{Cat.-Amb}(T_{Cat.} - T_{Amb.})$. Note that $\dot{m}$ and $\hat{H}_{In}$ strongly influence the value of T_{Cat}. The engine speed and residual fraction affect $\dot{m}$ and $\hat{H}_{In}$ respectively. The effects are illustrated in Figures 2.18 and 2.19.

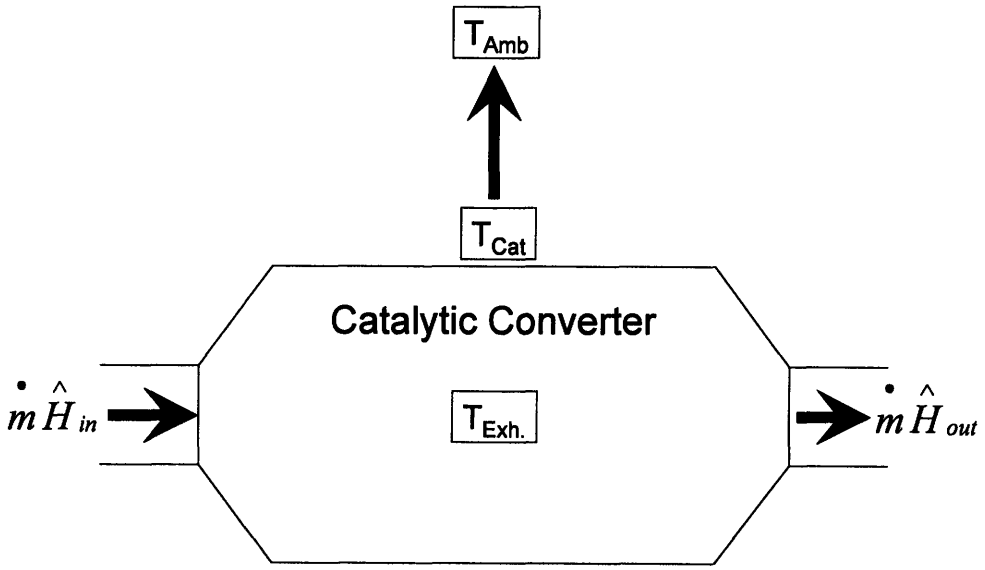

Figure 2.17: Heat Transfer Schematic of the Catalytic Converter

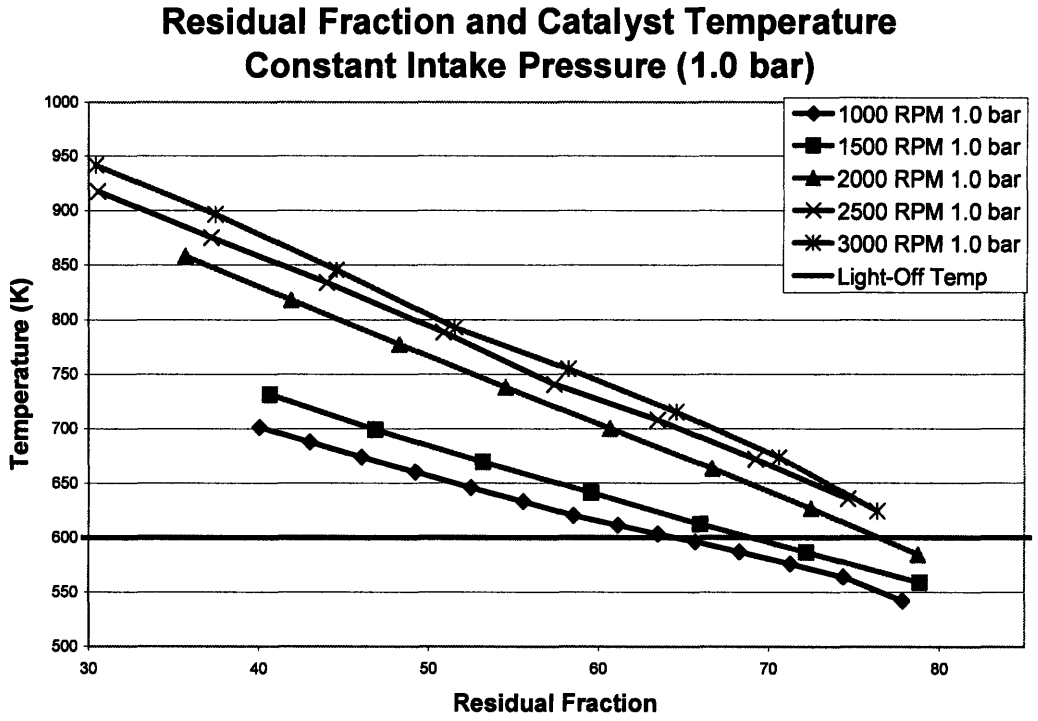

Figure 2.18: Residual fraction and catalyst temperature with varying speeds

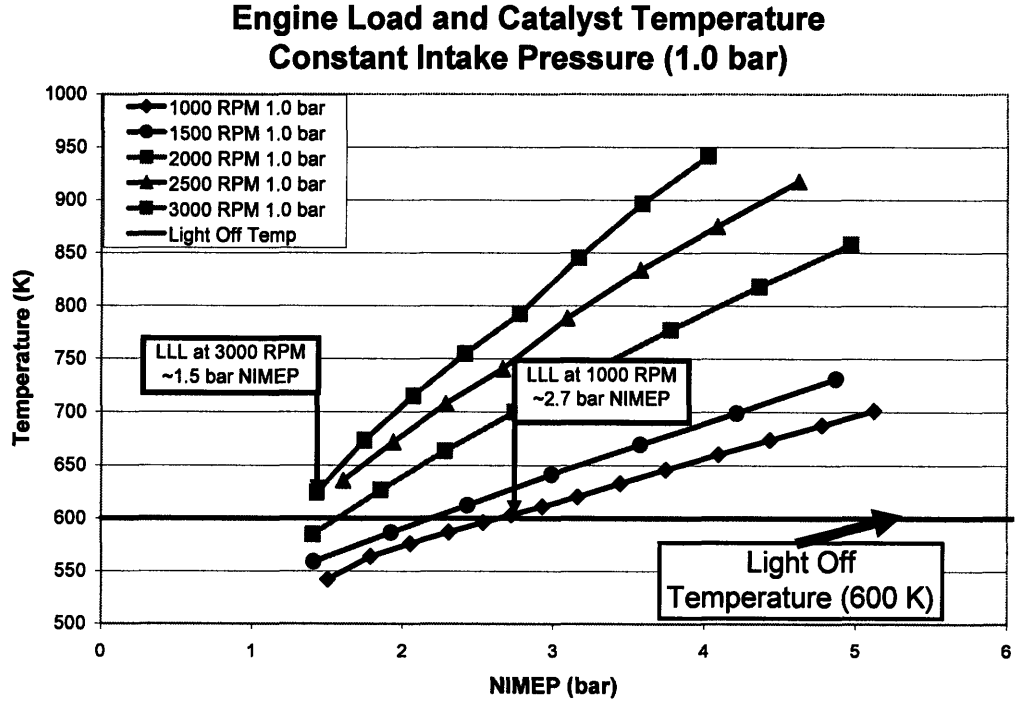

Figure 2.19: Engine load and catalyst temperature with varying speeds

2.8.2 Effects of Intake Pressure:

As described above with the effects of engine speed, it is the mass flow rate of the gasses which has the greatest effect on the catalytic converter's temperature. The temperature increases with increasing intake pressure at a constant engine load or residual fraction (figures 2.20 and 2.21) due to the increased mass flow rate at a constant engine speed occurring from a greater intake air density.

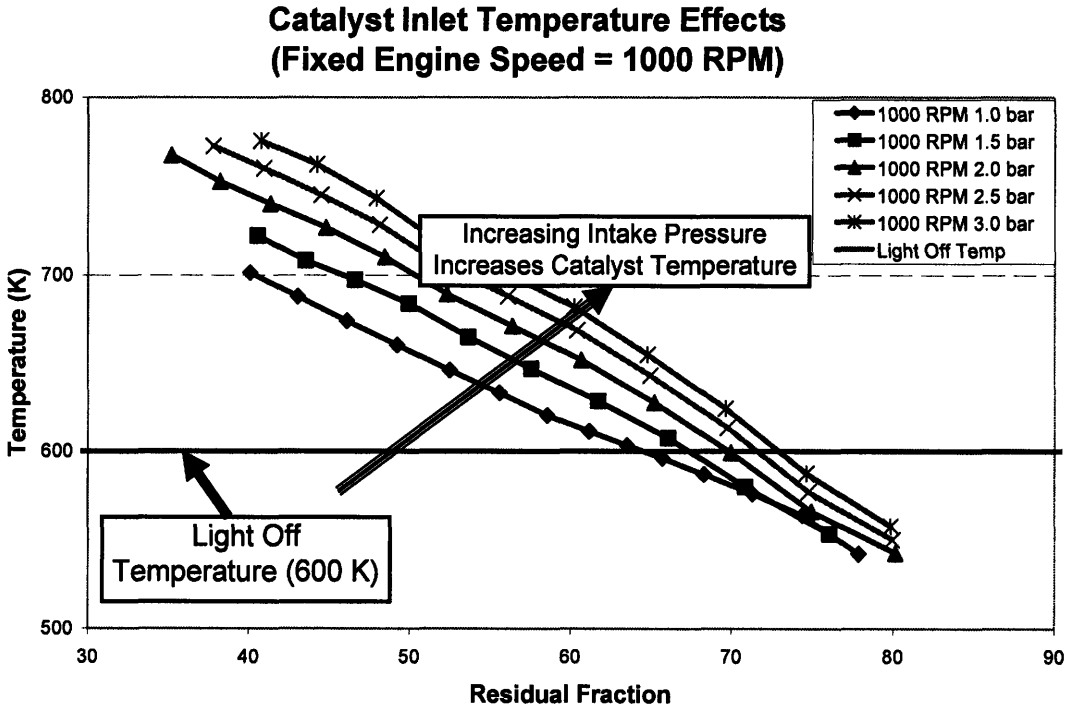

Figure 2.20: Residual fraction and catalyst light-off temperature with varying intake pressures (1 – 3 bars) at a constant engine speed (1000 RPM)

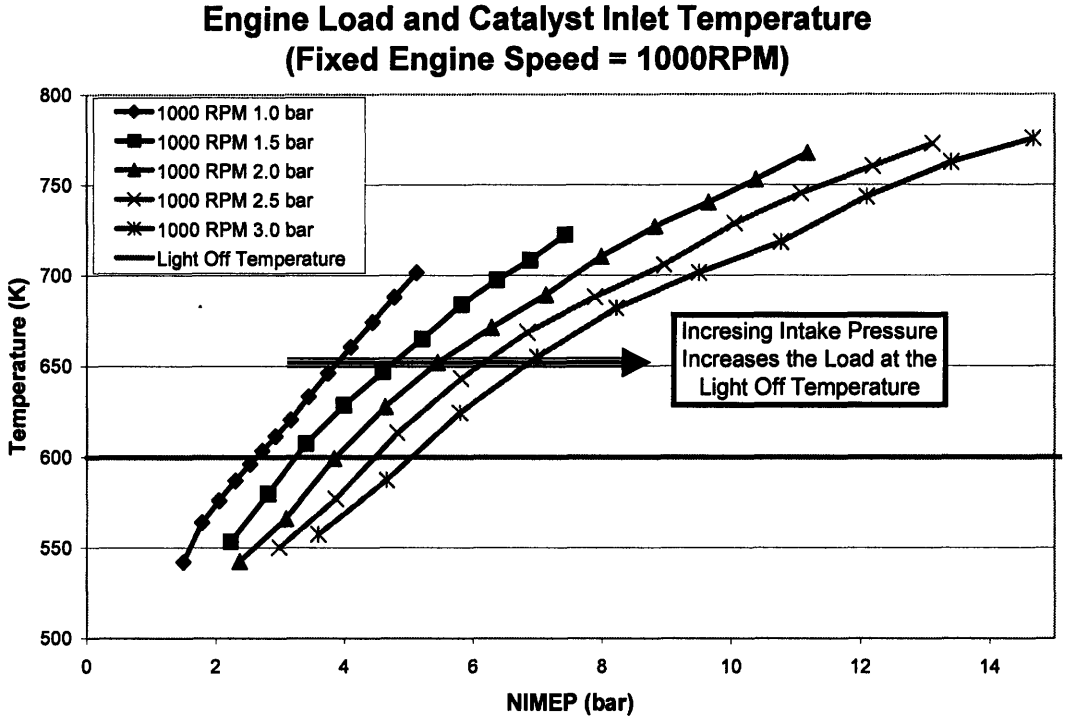

Figure 2.21: Engine load and catalyst light-off temperature with varying speeds

2.8.3 LLL at the Catalytic Converter Light-Off Temperature:

As explained in the previous two sections the lowest load at the 600 K light-off temperature occurs at the lowest intake pressure and at the highest engine speed. Often times it is not desirable from a fuel economy standpoint to have the engine running at a higher rpm. That is why on Figure 2.19 there are two limits noted, one at ~1.5 bar NIMEP (3000 RPM) and the other at ~2.7 bar NIMEP (1000 RPM). This is a large difference and could possibly be a disadvantage when developing an engine map for maximum fuel economy especially at idle conditions. This simply provides more motivation for the development of hybrid SI-HCCI engines where the SI handles the lower and upper loads and HCCI only operates at mid-load.

2.9 Combining the HLL and the LLL:

The combination of the two ideas of HLL and LLL together, and implementing a three way catalyst emissions reduction system, creates practical boundaries of operation for the system modeled. The catalyst conversion efficiency was chosen at 90%, a conservatively low value since modern catalysts operates at greater than 99% conversion efficiencies for NO_x. With this new limit the lowest limits possible are still achieved at the highest engine speeds at the lowest intake pressure, while the highest limits achieved are at the lowest speeds and at the greatest levels of boost. Figures 2.22 and 2.23 show off the load variation for a spread of values at the new HLL and at the LLL. For the range of values used in this simulation the absolute theoretical boundaries then become ~1.5 bar NIMEP to ~8.9 bar NIMEP (for a 90% efficient catalyst, NO_x=1.3g/kg fuel). These of course are only the theoretical limits where as the actual HCCI combustion will determine if these load values are actually able to be achieved, but it does provide a glimpse as to the maximum potential of HCCI in a modern application.

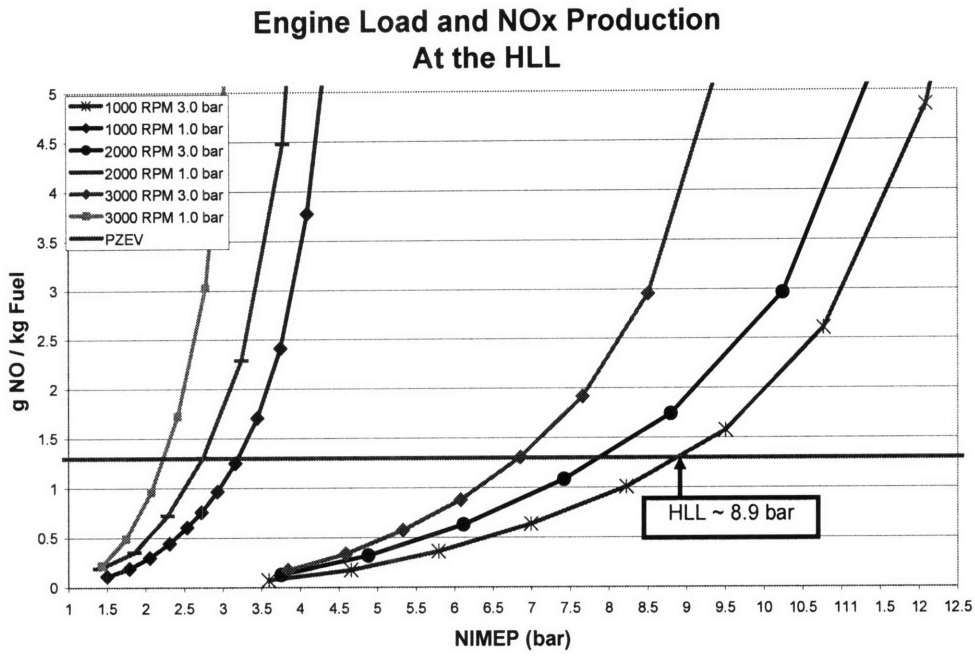

Figure 2.22: Engine load and NOx production at the PZEV limit with a 90% efficient catalyst at a variety of conditions

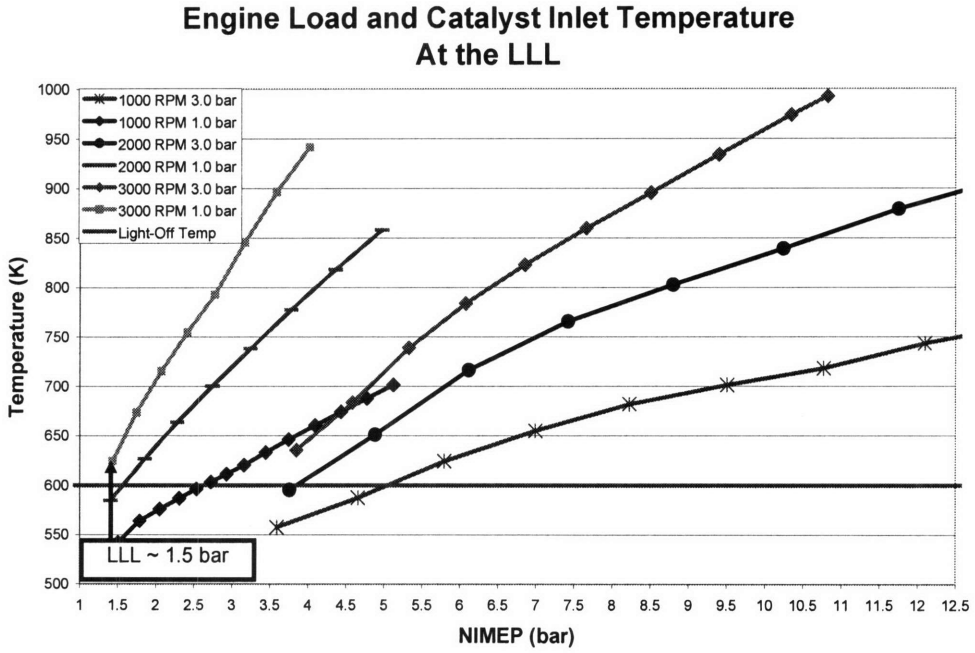

Figure 2.23: Engine load and catalyst inlet temperature at the catalytic converter light-off temperature at a variety of conditions

2.10 Burn Duration Simulations:

The effects of varying combustion duration and phasing on the performance of the engine were assessed. With HCCI, the combustion burn duration is much shorter than that of a standard SI engine; the start of combustion also occurs closer to top center. One of the difficulties with HCCI is that the combustion phasing, which can be characterized by the point at which 50% of the mass of fuel is burned, is hard to control. Also, in line with the theme of the overall project, different fuels have different auto-ignition characteristics and therefore have different burn durations and combustion-phasings. The model was used to see how much affect the changes in the phasing had on the engine's performance.

2.10.1 Model Setup:

The simulation described in the previous sections was used in this study. A single operating point was chosen with the speed (1500 RPM) and residual fraction (70%) both held constant for changes made to the combustion phasing and duration. The residual fraction was controlled by doing a symmetric valve timing sweep to find the desired timing to yield 70% residual fraction. The combustion phasing was tested by setting the parameters of the Weibe function. The CAD50 was set and then the burn duration was varied from 10 – 40 CAD in 5 CAD increments. This was also done for CAD50 varied from -1 – 19 CAD again in 5 CAD increments.

2.10.2 Results:

The results from the simulation were divided up into two main categories, effects of burn duration and effects of CAD50. Since the fuel burned for cycle was not held constant because of the changes in valve timing, and thus air intake, to maintain the 70% was not held residual fraction. The results were, therefore, normalized by calculating the gross indicated fuel conversion efficiency of the cycle. This measured how well the fuel delivered was converted to workable energy. All of the measurements and values are take as (and labeled as) gross values. This simply means that the pumping loop losses (intake and exhaust strokes) are not included in the work calculation, but only the compression and expansion stroke are examined. Equation 2.1details how the measured GIMEP was converted to the gross indicated fuel conversion efficiency.

Equation 2.1: Gross indicated fuel conversion efficiency

$$\eta_{f,ig} = \frac{GIMEP(Pa) \cdot V_D(m^3) \cdot N(rev/\sec)}{n_R(rev/cyc) \cdot \dot{m}_f(kg/\sec) \cdot Q_{HV}(J/kg)}$$

$GIMEP(Pa)$ - Gross indicated mean effective pressure (Pa)
$V_D(m^3)$ - Displaced volume (m^3)
$N(rev/\sec)$ - Engine speed (rev/sec)
$n_R(rev/cyc)$ - Number of revolutions per cycle (rev/cyc)
$\dot{m}_f(kg/\sec)$ - Fuel mass flow rate (kg/sec)
$Q_{HV}(J/kg)$ - Lower heating value of the fuel (J/kg)

Figures 2.24 and 2.25 illustrate the effects of changing the burn duration on $\eta_{f,ig}$ at selected values of CAD50. Figure 2.24 shows the absolute fuel conversion efficiency and each of the lines shown is a different CAD50. It is clear that the longer the burn duration the lower the conversion efficiency. This is because the fuel's energy is spread

out over decreasingly effectively cylinder positions. The ideal Otto cycle involves constant volume heating, which would involve all of the fuel's energy to be released instantaneously when the piston was at the top cylinder position. Energy released after the piston reaches the top position is utilized less efficiently because there is less left in the expansion stroke to extract work from the hot gasses. If the energy is released before the top position then it creates more work during the compression stroke, so not only is the fuel's energy not used as efficiently as it could it is also being used to create more negative work for the system. This is why the engine becomes more inefficient as the burn duration increases.

Sometimes it is also helpful to look at normalized plots (efficiency is normalized by the value of the 10-90 burn duration of 10°CA) to help compare amongst the different CAD50. Figure 2.25 presents the normalized plots and it shows that despite the CAD50 changes the plots still follow the same shape and roughly undergo the same percent change in efficiency. Despite a 30 CAD increase in burn duration for each combustion phasing, the gross efficiency only decreased 4 to 5 percent depending upon the phasing selected. In more absolute terms the drop between the maximum and minimum efficiencies is from 40.5% to 37%, this is about an 8.5% change, but this is a combination of both efficiency drop from both the burn duration and the combustion phasing.

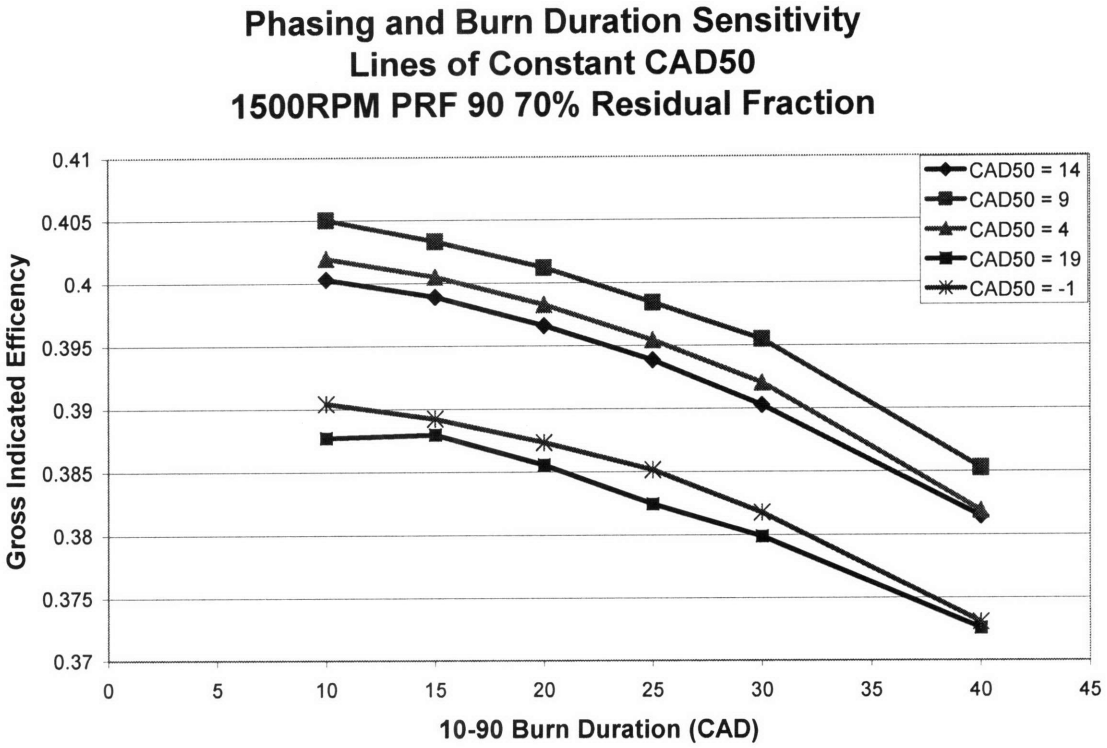

Figure 2.24: Efficiency effects of burn duration at constant combustion phasing (CAD50)

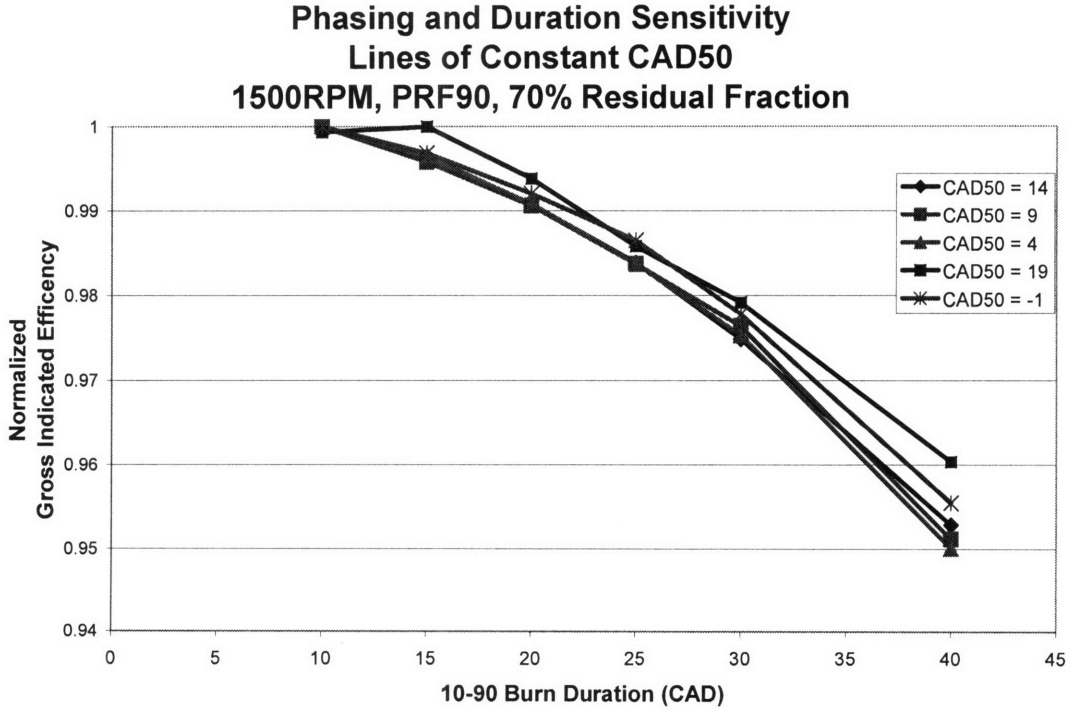

Figure 2.25: Normalized effects of burn duration at constant combustion phasing (CAD50)

Figures 2.26 and 2.27 illustrate the effects of the opposite case when the burn duration is held constant and the combustion phasing is varied. Instead of a straight decline like was shown with the varied burn durations, the varied combustion phasing appears as a dome shape. This means that there is a phasing which has the peak efficiency and that deviating from that phasing causes a decrease in the cycle's efficiency. Normalizing the curves about their local maximum value produces figure 2.27. The normalization shows that the plots all still have the same shape and collapse onto each other. Also it shows that shapes of the curves are approximately parabolic and that the center of each curve is approximately 7-9 CAD after top dead center (ATDC). The deviation of CAD50 in this range causes approximately a 3.5 – 4 % decrease in efficiency. This combined with the 4 – 5 % decrease caused by the burn duration effects leads to the overall ~8.5% decrease calculated from the maximum and minimum efficiencies of 40.5 and 37%. What this analysis really shows is that even for large changed in burn duration even to levels associated with SI combustion, there is a small change at a constant phasing. The phasing also shows similarly small decreases in efficiency over a wide range of values, but the one important point to remember is that the shape of the lines of constant burn duration are parabolic. This means that slope of those lines will get larger and larger as the phasing moves away from the maximum. So while this range of points only has a small variation of values, any derivation outside of that range will cause a much greater decrease in efficiencies.

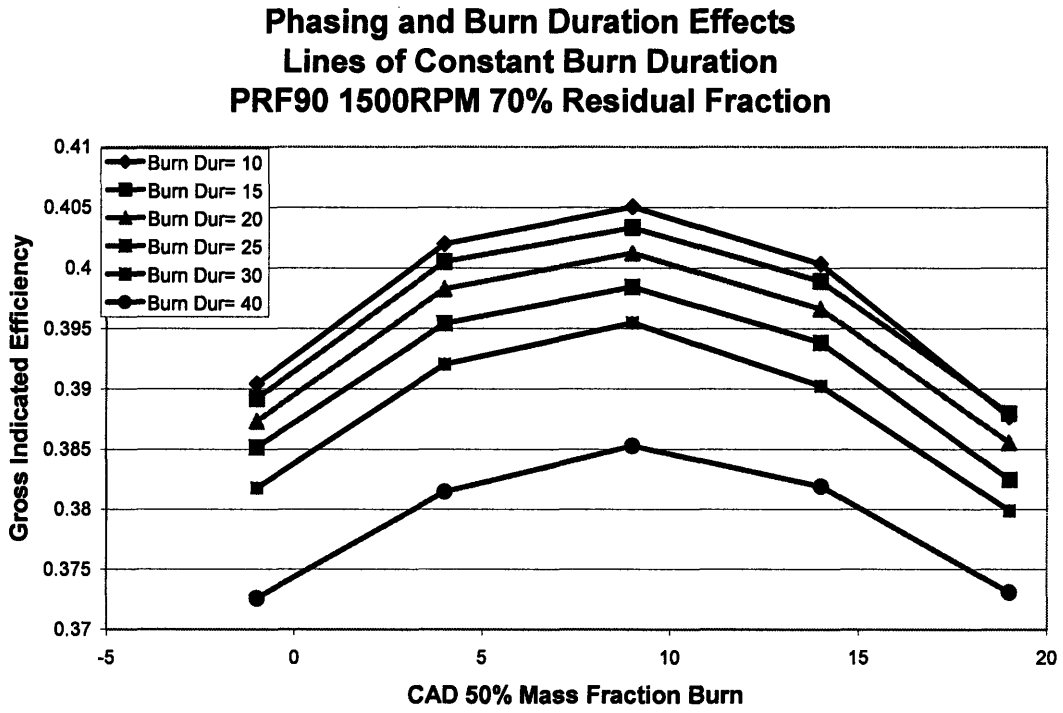

Figure 2.26: Efficiency effects of combustion phasing (CAD50) at constant burn durations

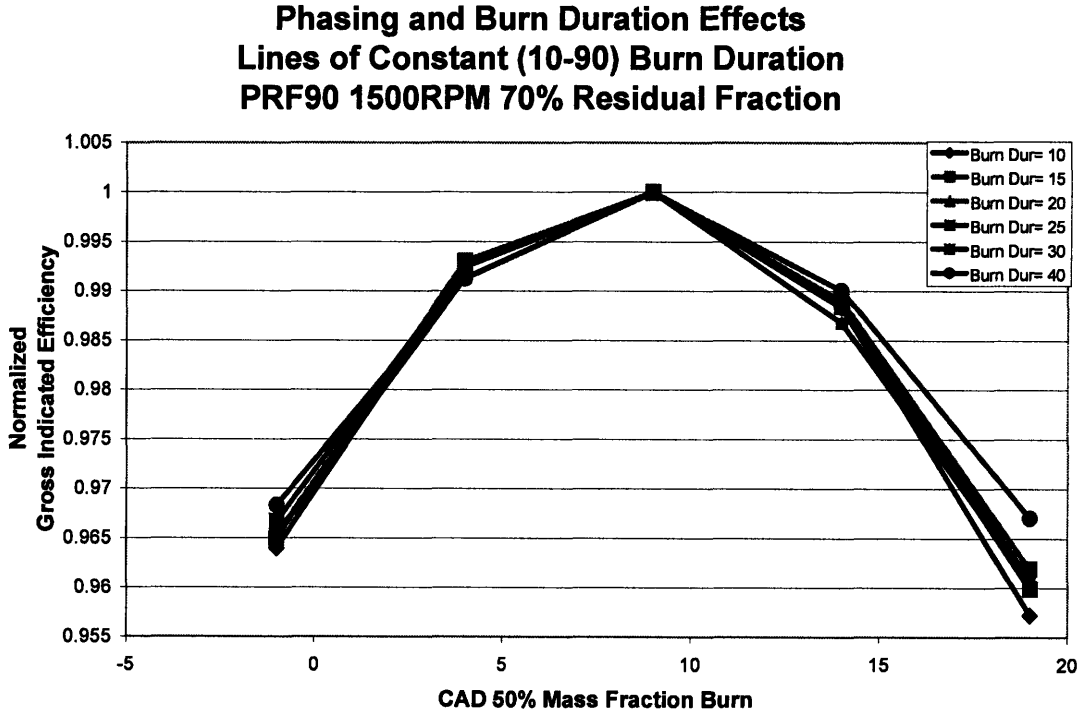

Figure 2.27: Normalized effects of combustion phasing (CAD50) at constant burn durations

3 Fuel Comparisons at the HLL

Previous research at the Sloan Lab was done to asses the fuel effects on the high load and low load combustion limits of HCCI engines. The range of fuels tested was based upon the variations found in the North American marketplace [7]. The results demonstrated that for the range of fuel compositions existed in the marketplace, the impact of fuel variations was modest for both limits. To confirm this result, a much wider variation in fuel properties than the market fuel was tested here. The fuels PRF90 and PRF60 were used to accentuate the fuel effects on the two limits. It was hoped that the two fuels, with very different auto-ignition characteristics, would provide insight into how combustion limits were affected.

3.1 Fuel System:

The focus of these experiments was to examine the effects of fuel composition on HCCI combustion. A schematic of the fuel system is shown in Fig. 3.1. The main goal was to make sure that the fuels remained separate at all times and that the fuel that the engine was receiving was definitely only one fuel and that it was not mixed with any others. That is one of the reasons that a nitrogen purging system was introduced. This system would allow for an inert gas to push the fuel from the inlet hose and fuel rail cleanly and without wasting any additional fuel. The new fuel could then fill the clean rail and be ready to use without contamination.

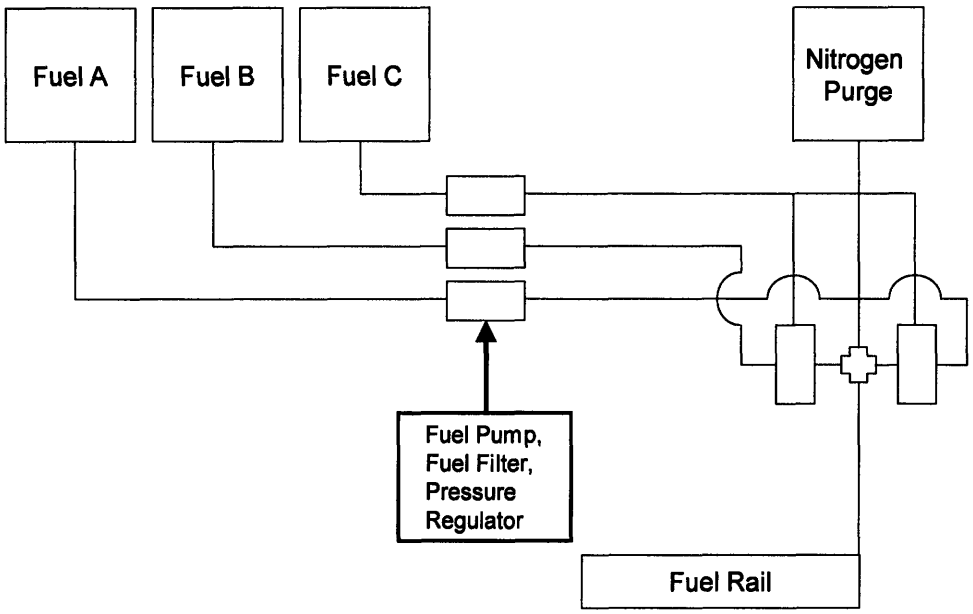

Figure 3.1: Fuel System Schematic for three fuel switching

3.2 Air Conditioning:

To minimize the effects of atmospheric ambient conditions on combustion, the air entering the cylinder was first conditioned. The ambient air is pulled in through a filter and then enters a cooler. The purpose of the cooler was to lower the air's temperature and condense the water vapor in the air out so that the air was completely dry when entering the cylinder. Next, the air travels through a heater which raises the temperature to 40 °C as the air flows to the intake port. This way, the air that enters the cylinder, is always at the same atmospheric conditions removing any variables associated with lab conditions.

3.3 Instrumentation:

To record the performance of the engine there is a great deal of instrumentation involved. The LabVIEW [12] data acquisition package was used to record and sort the engine performance in the same manner as previous researchers [7,11]. However, not all of the instrumentation was used again, and the sensors that were used are listed in Table 3.1. The pressure transducer was used to monitor the pressure trace and to calculate GIMEP, NIMEP, PMEP, CAD50, and the maximum $dP/d\theta$. The MAP was used to make accurate pressure trace comparisons, while the intake and exhaust cam position sensor were used as a check to make sure that the cams were performing in the desired fashion. The spark was monitored, but the data was not recorded because the spark was only used to start the engine and was not part of the research. Fuel pulse width combined with the fuel-air ratio provided the fuel of the amount of incoming fuel and air. The fuel injectors were calibrated at the beginning of the experiments and the calibration curve is presented in the appendix. So, while the exact fuel mass was never calculated the relative fuel mass was monitored through the fuel pulse width while maintaining a relative air-fuel ratio (λ) of 1. The same meter which was used to calculate the fuel-air ratio was also used to calculate the NO_x concentration in the exhaust gases. The NO_x meter is accurate to approximately $\pm$30ppm of NO_x while some the highest values that were recorded only registered around 100ppm, so even though the values were recorded there is a great deal of error associated with them. Finally, there were several thermocouples used throughout the engine to record temperature. One of the most important measurements was on the exhaust gases. The temperature fluctuation in the exhaust gas would indicate when a stable operating point was reached and when it was stable enough to record the data.

Many of the other thermocouples were used in feed back systems to keep the systems at ideal temperatures such as the inlet air temperature and engine cooling system.

Cylinder pressure (Kistler 6052b sensor)
MAP (Omega PX 176 sensor)
Intake cam position (modified production sensor)
Exhaust cam position (modified production intake cam sensor)
Spark
Fuel pulse width
Fuel-Air ratio (Horiba MEXA 720NOx – combined air-fuel ratio & NOx sensor)
NO_x (Horiba MEXA 720NOx – combined air-fuel ratio & NOx sensor)
Temperature (Omega Thermocouple)

Table 3.1: List of sensors and their uses [7]

3.4 Experimental Procedure:

As mentioned before the intake system was modified so that air at a constant temperature and relative humidity would be delivered to the engine. Also, there was an external engine coolant heating/cooling system was devised so that the engine would be maintained at a constant 90°C (±2°C). It was necessary to have the engine warmed up for starting. Below are listed the steps in acquiring data for a typical data point.

1) Warm the engine up to 90°C
2) Using the Motor and the Dynamometer, run the engine up to the desired speed
3) Adjust the intake air temperature so that it is operating at 40°C
4) Using the engine controller select a middle valve timing (usually exhaust valve close (EVC) 93 CAD before TDC and intake valve open (IVO) 93 CAD after TDC)
5) Apply the desired fuel pulse width and turn on the spark and adjust spark timing

6) Turn on the fuel injectors and get the engine to fire (this may take several attempts)
7) Once the engine is firing adjust the fuel pulse width so that $\lambda=1$ and let the engine reach a stable operating point (exhaust gas temperatures stabilize)
8) Once the combustion is stable move the engine towards the starting point (usually EVC and IVO are >100 CAD before and after TDC respectively) while till maintaining $\lambda=1$
9) Once the engine is stable again at the new valve timings the spark can be turned off and the engine will need to re-stabilize
10) Once stable record a data point
11) After the data collection has finished advance the timing (move EVC and IVO closer to TDC) by 1 CAD, adjust the fuel pulse width to maintain $\lambda=1$, and let the combustion stabilize, let the engine run for approximately 5 min, the collect the data
12) Repeat step 11 moving EVC and IVO closer (keeping symmetric timing) and closer to TDC increasing the load. The HLL is reached once one of two limits is reached either the maximum pressure rise rate is greater than 5 MPa/ms [7] or combustion is not longer to sustain itself (misfire)

As briefly mentioned in step #12, there are two limits associated with the HLL of combustion for HCCI. The first one that was listed was the maximum pressure rise rate of 5 MPa/ms. This value was chosen as something analogous to the knock limit in SI engines. It was determined [7] that pressure rise rate greater than this value would yield unacceptable NVH. The second limit is the misfire limit. The engine can misfire at both

the high load and low load limits. At the HLL the misfire is due to the insufficient trapped residual gasses inside of the cylinder. Without enough trapped enthalpy the incoming charge will not be able to ignite. In comparison, the LLL is determined by the temperature of the residual gases. There is enough gas trapped, but the gas is not hot enough because the previous cycle's energy was not enough to raise the residual gasses temperature high enough to ignite the next cycle. The above steps are repeated several times to verify which limit occurs and at what load.

3.5 Results:

The list matrix consists of two speeds (1000 and 1500 RPM) and three different fuels (PRF60, PRF 90, Extremely Low Aromatic and Olefin Blend (ELAO)). The initial goal was to find the HLL at each of these conditions and to compare them with each other to see what effect the fuel properties had on the limit. Figures 3.2 and 3.3 show the performance of PRF 60 as it approaches the HLL.

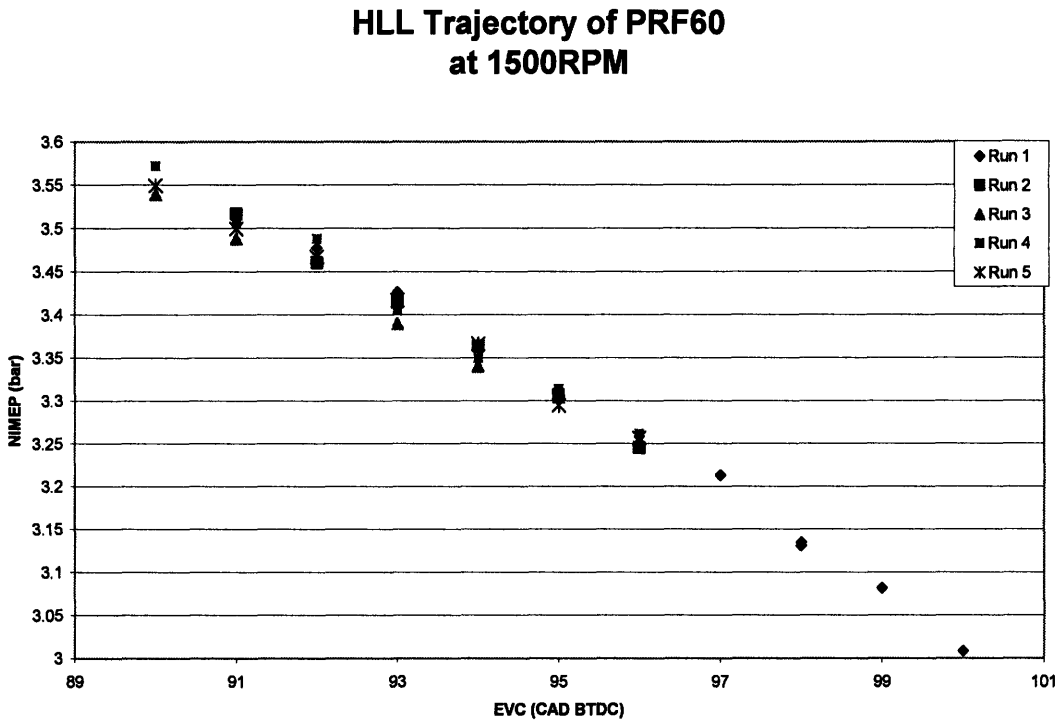

Figure 3.2: HLL Trajectory of PRF60 with varying Exhaust valve timing at 1500RPM

Figure 3.2 shows what happens to the engine's performance as the EVC timing is moved closer and closer to TDC (retarding EVC). As EVC approaches TDC the gas exchange process traps less and less residual fraction which in turn allows in more and more fresh charge which allows for greater load to be achieved. PRF60 did not misfire, and actually it reached the pressure rise rate very quickly. Examining the plot of engine load vs. exhaust timing is not helpful in determining the value of the high load limit, rather the engine load vs. the maximum pressure rise rate ($dP/d\theta$) must be examined. Figure 3.3 shows this relationship and shows that for this operating range as the engine load is increased (residual fraction decreased) the maximum pressure rise rate increases also. As shown in figure 3.3 this leads to the fuel being pressure rise rate limited at a NIMEP of ~3.45 bar.

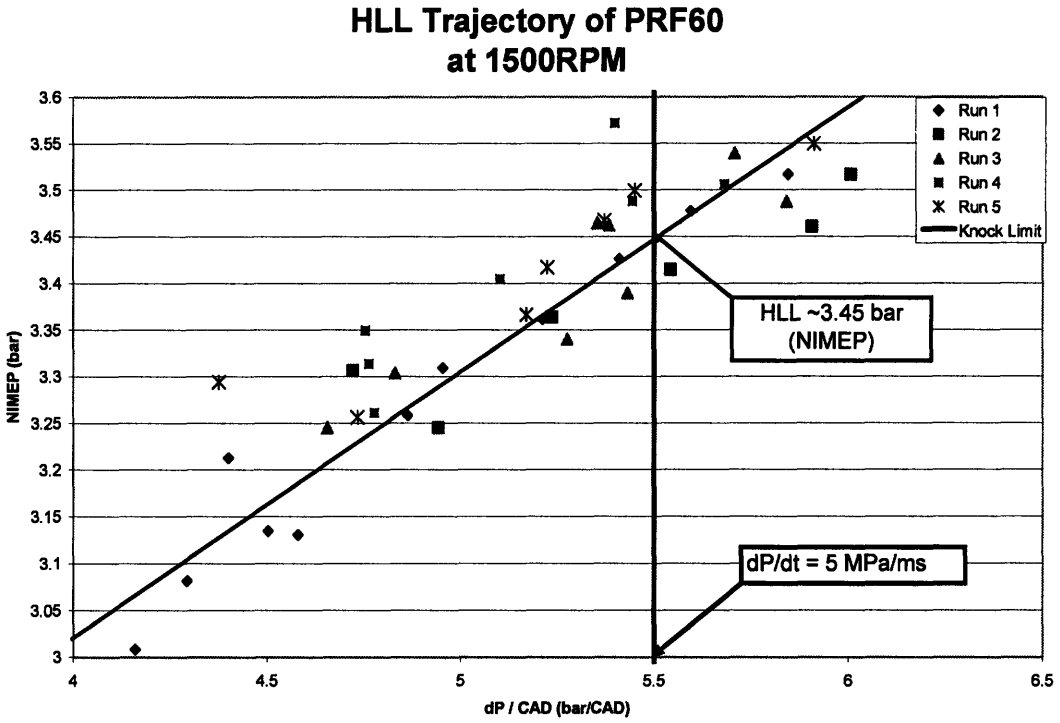

Figure 3.3: HLL Trajectory of PRF60 against maximum pressure rise rate at 1500RPM

At the same speed (1500 RPM) PRF90 was run using the same procedure as listed above and it produced Figures 3.4 and 3.5. The HLL with PRF90 was reached by misfire instead of being knocked limited. The types of limits were not the only aspects that were different, but how the maximum pressure rise rate behaved as the fuels reached their limits was also different. As the engine load was increased the maximum pressure rise rate actually decreased, whereas in the case of PRF60 the maximum pressure rise rate increased. The pressure rise rate continued to decrease all the way until the engine misfired and thus signaled the HLL which occurred at ~3.8bar.

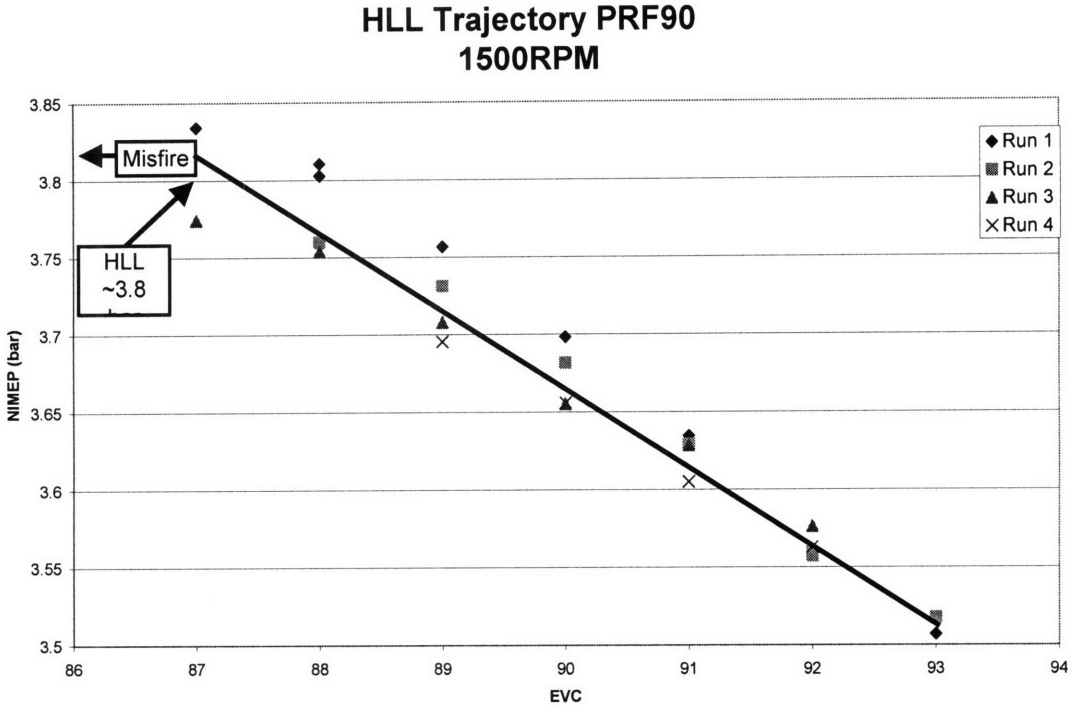

Figure 3.4: HLL Trajectory of PRF90 with varying Exhaust valve timing at 1500RPM

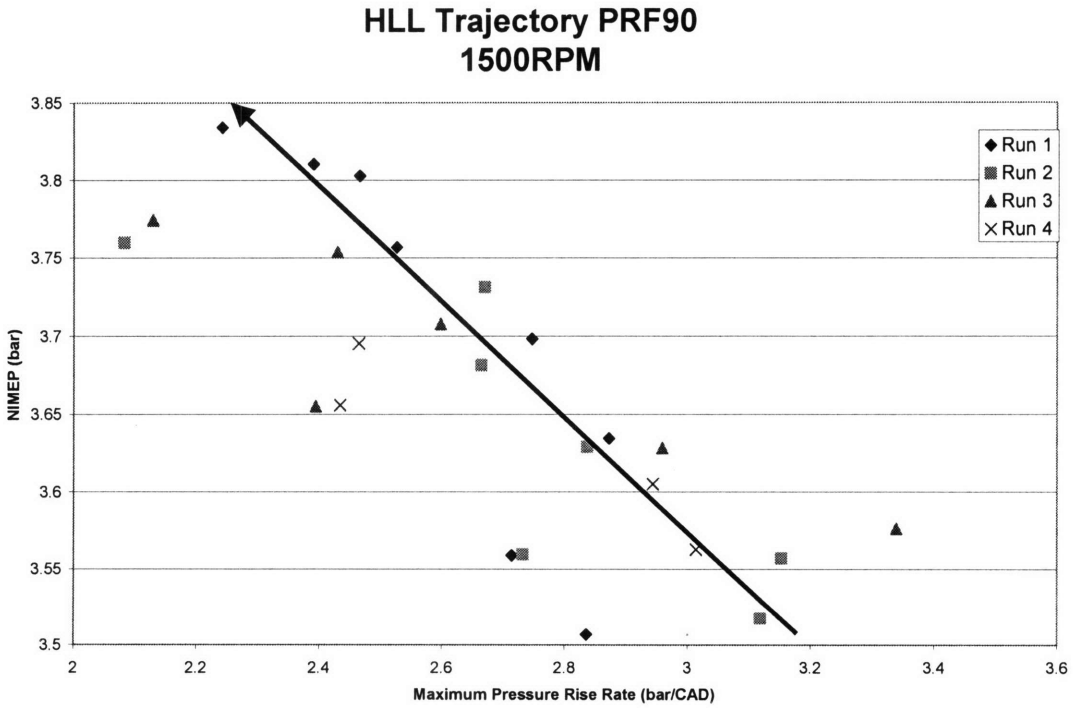

Figure 3.5: HLL Trajectory of PRF90 with maximum pressure rise rate at 1500RPM

Figures 3.6 and 3.7 illustrate the HLL trajectories for the ELAO market fuel blend. This fuel, like PRF90, was limited by misfire instead of by the maximum pressure rise rate. This fuel had the highest HLL of the three fuels at 1500RPM with a NIMEP of ~3.95 bar. The most interesting part of this analysis is shown in figure 3.7. The maximum pressure rise rate exhibited both an increase and decrease in maximum pressure rise rate with an increase in engine load. This makes it seem like it performs like both PRF90 and 60, but in the end was misfire limited like PRF90. This combination of fuel effects will be discussed in the next section.

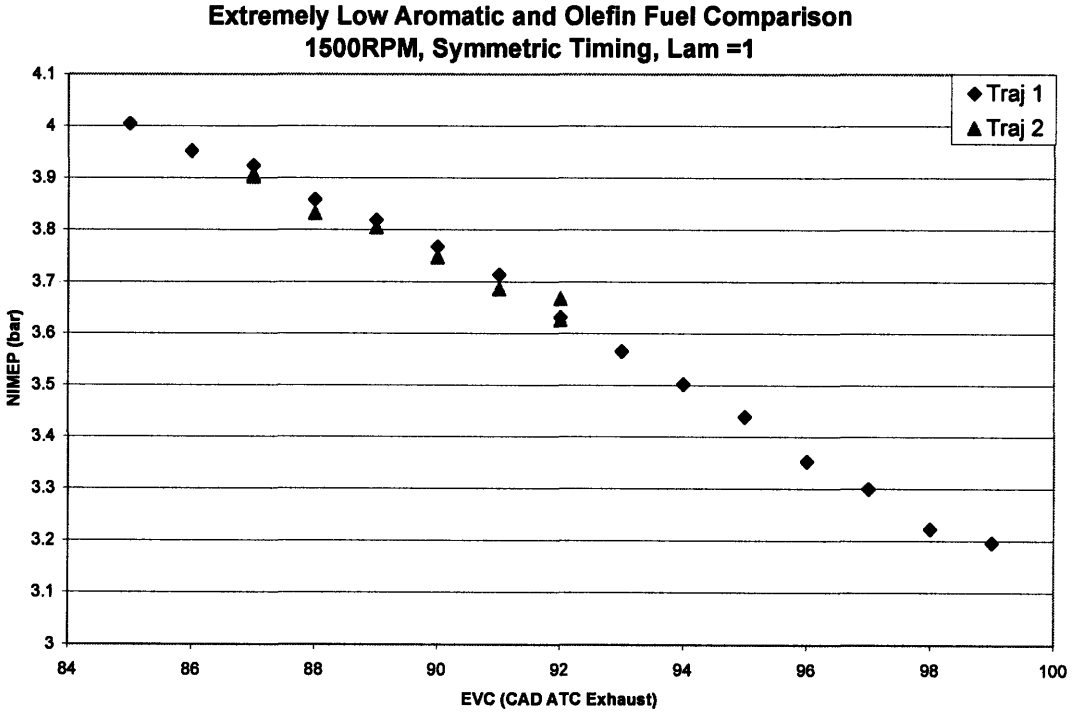

Figure 3.6: HLL Trajectory of ELAO with varying Exhaust valve timing at 1500RPM

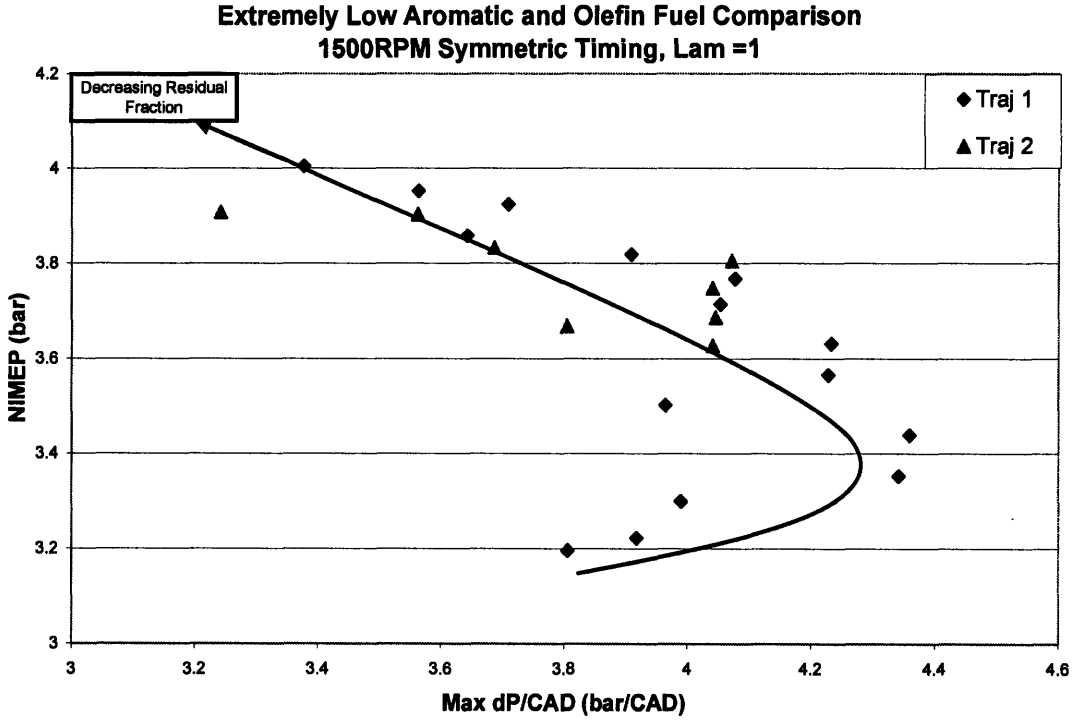

Figure 3.7: HLL Trajectory of ELAO with maximum pressure rise rate at 1500RPM

Once the results for 1500 RPM were completed, the effects of speed on the HLL were attempted to be analyzed. The engine speed was reduced to 1000 RPM and the new HLL was determined again using PRF60 first. Figures 3.8 and 3.9 are the same types of plots as before, but at the new speed. The most important factors are that the new speed allows for greater air flow into the cylinder thus a higher load can be achieved at the same amount of dilution, thus leading to a higher HLL which is now ~3.92 bar whereas 1500 RPM had a HLL of ~3.45 bar. Also, PRF60 still exhibits the same behavior as 1500 RPM, where the maximum pressure rise rate increases with increasing load, which leads to the fuel being limited by the pressure rise rate and not by misfire.

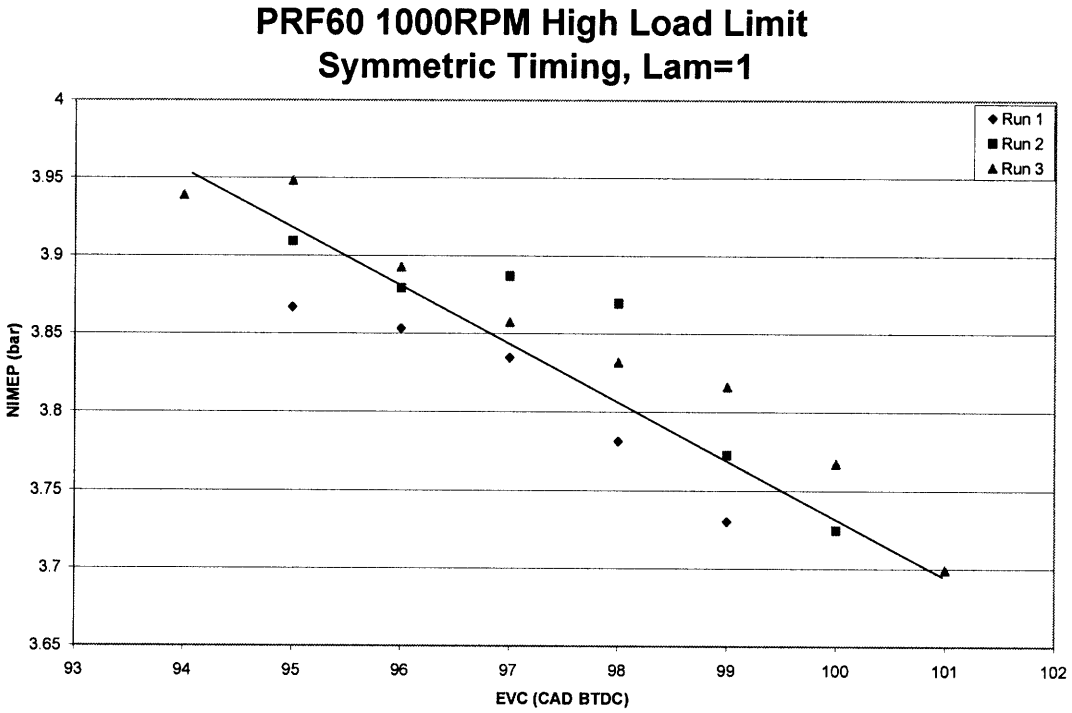

Figure 3.8: HLL Trajectory of PRF60 with varying Exhaust valve timing at 1000RPM

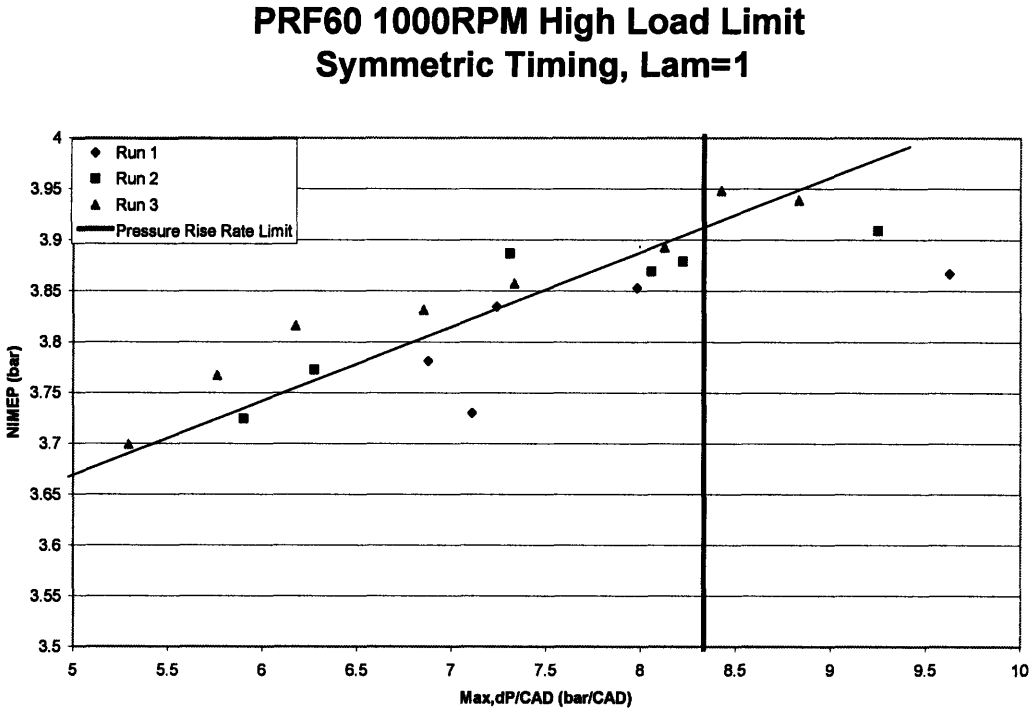

Figure 3.9: HLL Trajectory of PRF60 with maximum pressure rise rate at 1000RPM

It was attempted to run PRF90 at 1000RPM but the limited auto-ignition characteristics of the fuel reduce its operating range. However it was able to be tested at 1300 RPM. A similar phenomenon was observed with PRF90 as was with PRF60. The lower speeds increased the load at the limit, but did not affect which type of limit occurred. Figures 3.10 and 3.11 show the data collected at the reduced speed which yielded a HLL increase to ~4.05 bar, a .25 bar increase over the 1500 RPM HLL. An interesting point again occurred when examining Figure 3.11. The maximum pressure rise rate did not always decrease with increasing load. Although it is not as clear, as in Figure 3.7 with the ELAO blend, but it does appear to have a similar shape with both increasing and decreasing maximum pressure rise rate with increasing load. Finally, Figure 3.12 shows the comparison of the collected HLL data and plots the changes against the changes in engine speed. It is hard to compare these data points however

because of the limited number of points and the inability of PRF90 to run at 1000 RPM with PRF60. What is clear though is that running at a lower speed does increase the HLL and that it does not seem to affect which limit is reached.

NOTE: The lower speed testing was desired to include ELAO, but it was unable to be done due to both time and fuel availability constraints.

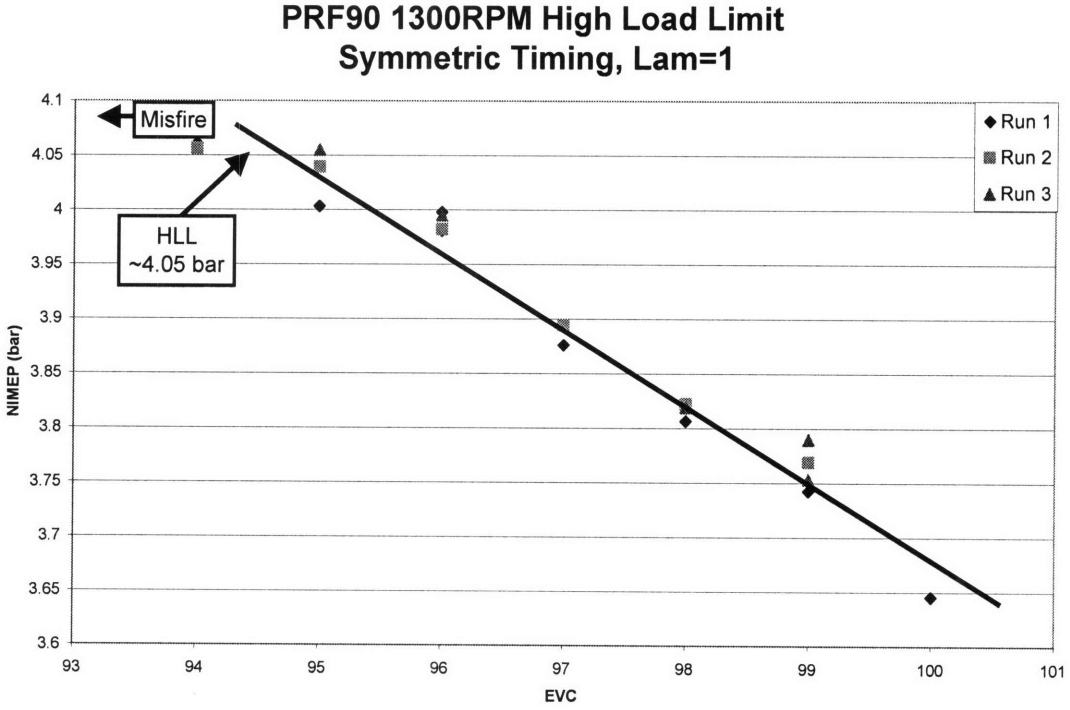

Figure 3.10: HLL Trajectory of PRF90 with varying Exhaust valve timing at 1300RPM

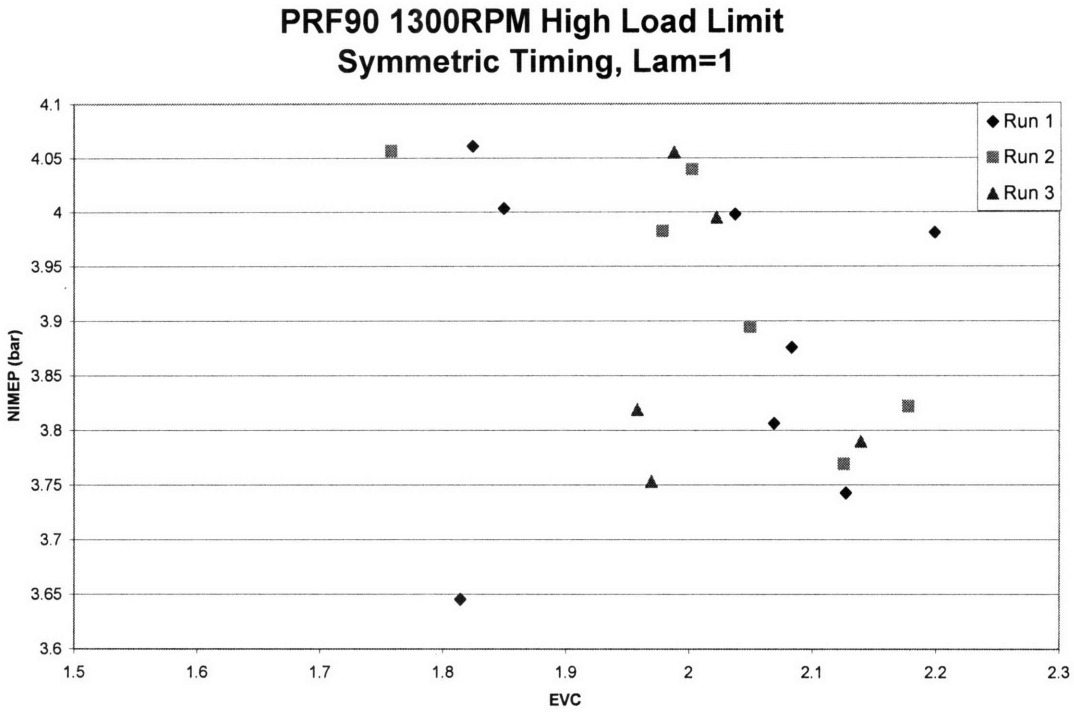

Figure 3.11: HLL Trajectory of PRF90 with maximum pressure rise rate at 1300RPM

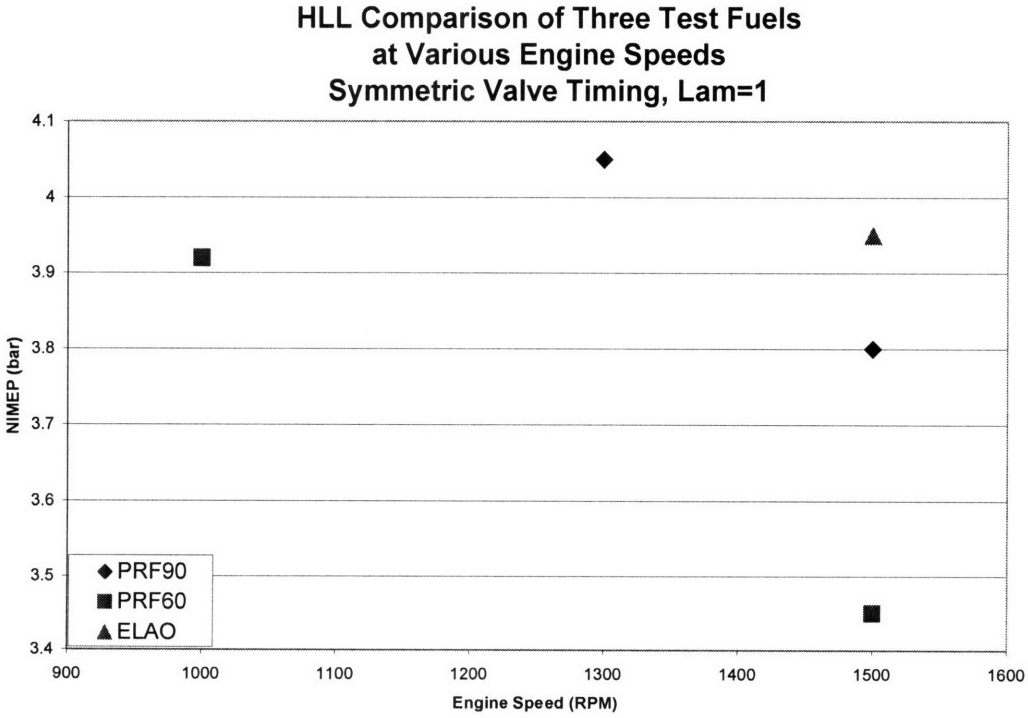

Figure 3.12: HLL comparison of the three fuels at the various speeds

3.6 Effects of Intake Valve Timing:

As mentioned above, an interesting scenario presented itself when PRF90 and PRF60 behaved very differently at 1500 RPM, but ELAO behaved a little bit like both fuels. Figure 3.13 illustrates how each fuel performs with relation to the maximum pressure rise rate and the engine load. Also, when the speed was reduced to 1300 RPM PRF90 began to show signs of the same phenomenon as ELAO. This also raises the questions related to previous research. Previous research [7] reported that at the HLL the pressure rise rate and misfire limit were very close to one another and essentially the HLL was both limits simultaneously. The results acquired by the present testing appear to show, that with symmetric timing, that the two limits are very distinct and separate from one another. Previous research [7] however did not run symmetric valve timing. It was shown that, in general, exhaust valve timing controls the load of the engine, while the intake valve timing controls the combustion phasing. Figure 3.14 shows that effects of changing the intake valve timing with a constant EVC. This is the same plot that is shown in Figure 3.7, except that the additional points are added. This was done by holding the EVC constant at 94 CAD BTDC and then moving the IVO from the symmetric position of 94 CAD ATDC and moving it closer and closer to TDC (making that number smaller). The main effect shown is that the when the IVO is moved closer to TDC the maximum pressure rise rate decreases. A smaller secondary effect is that, during the same movements of the intake timing the NIMEP is lowered slightly. This is counter intuitive, since the movement of IVO closer to TDC would also move the intake valve closing (IVC) closer to BDC, leading to less air being displaced during the compression stroke. This is most likely due to wave phenomenon in the intake port, and would be different at a different operating condition.

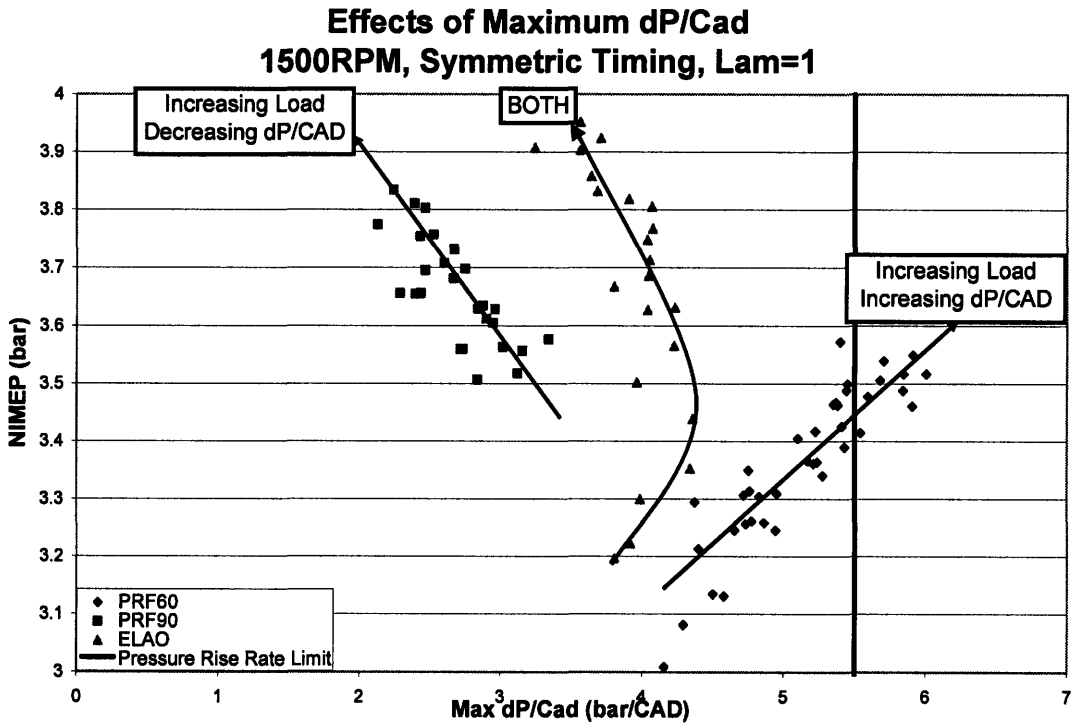

Figure 3.13: HLL Trajectory of the three test fuels against maximum pressure rise rate at 1500 RPM

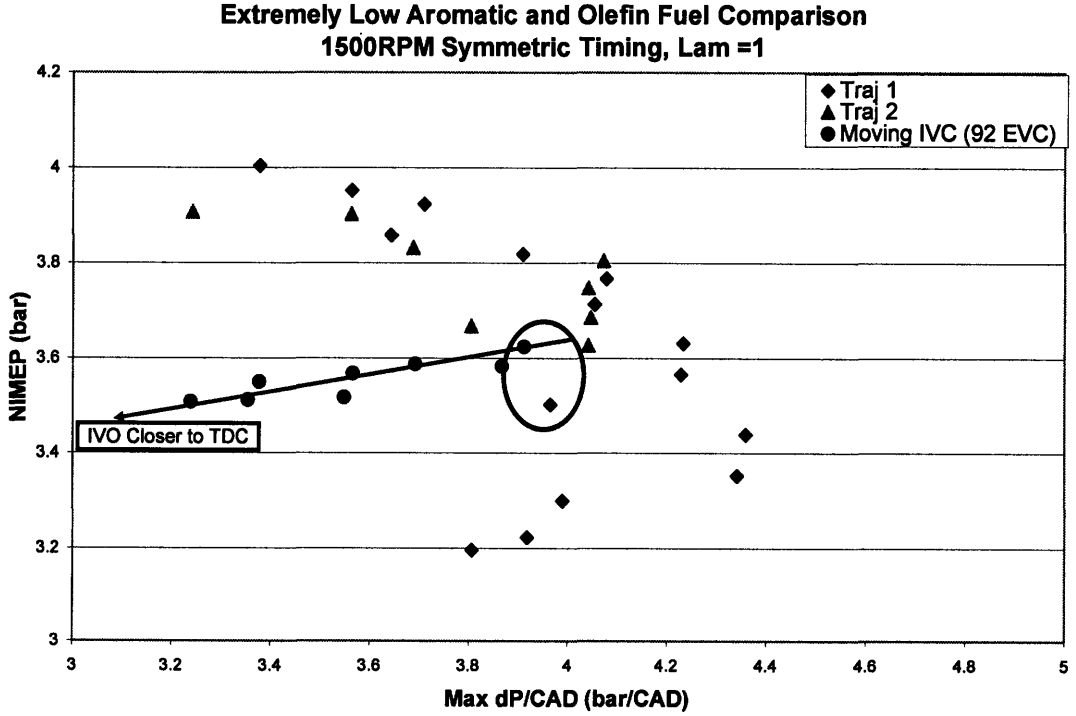

Figure 3.14: Effects of moving IVO closer to TDC at a constant EVC at 1500RPM

The symmetric valve timing constrain was removed to do the following: first, was to see if the PRF60 behavior could be made to have a curve similar to that of ELAO in Fig. 3.13, and second, to see if PRF60 exhibit both misfire and pressure rise rate limits as was described with other fuels in past research. Similar testing was also desired for PRF90 fuel, except in this case it was desired to try and get the fuel to reach the pressure rise rate limit, since it is misfire limited in the symmetric valve timing configuration.

PRF60 was first tested with the same procedure described above, except that the intake valve timing was changed. The change was indexed by sequencing to the symmetric valve timing with an offset. For example if an EVC timing of 98 CAD BTC was chosen and a -10 CAD offset was used the IVO timing would be 98-10=88 CAD ATC. With a negative offset value, the IVO is always closer to TDC than the EVC. Figure 3.15 shows PRF60 at six different intake valve timing offsets (symmetric, -5, -7, -10, -13, -15 CAD) over a wide sweep of exhaust valve timings (~25 – 30 CAD change in exhaust valve timings). If the symmetric timing is first examined and then the changes in timing are looked at from smallest to greatest offset, some basic trends exist. From symmetric to the -10 CAD offset, it appears that increasing the offset shifted the curves upward; thus the pressure rise rate limited NIMEP values (intersection of the limit line and the curves) decreases slightly (from 3.82 bar to 3.65 bar). At -13° and -15° offset, however the $dP/d\theta$ versus NIMEP curves shift substantially downwards. The curves also exhibit significant curvature. Note that the cam phasing changes only 3 CAD from offsets of -10° to -13°. It is observed that the trajectory of the EVC sweep at the -13° offset was close to the pressure rise rate limit, while the actual constrain was misfire

limited. It is conceivable taht both the pressure rise rate limit and misfire limit are in the same vicinity.

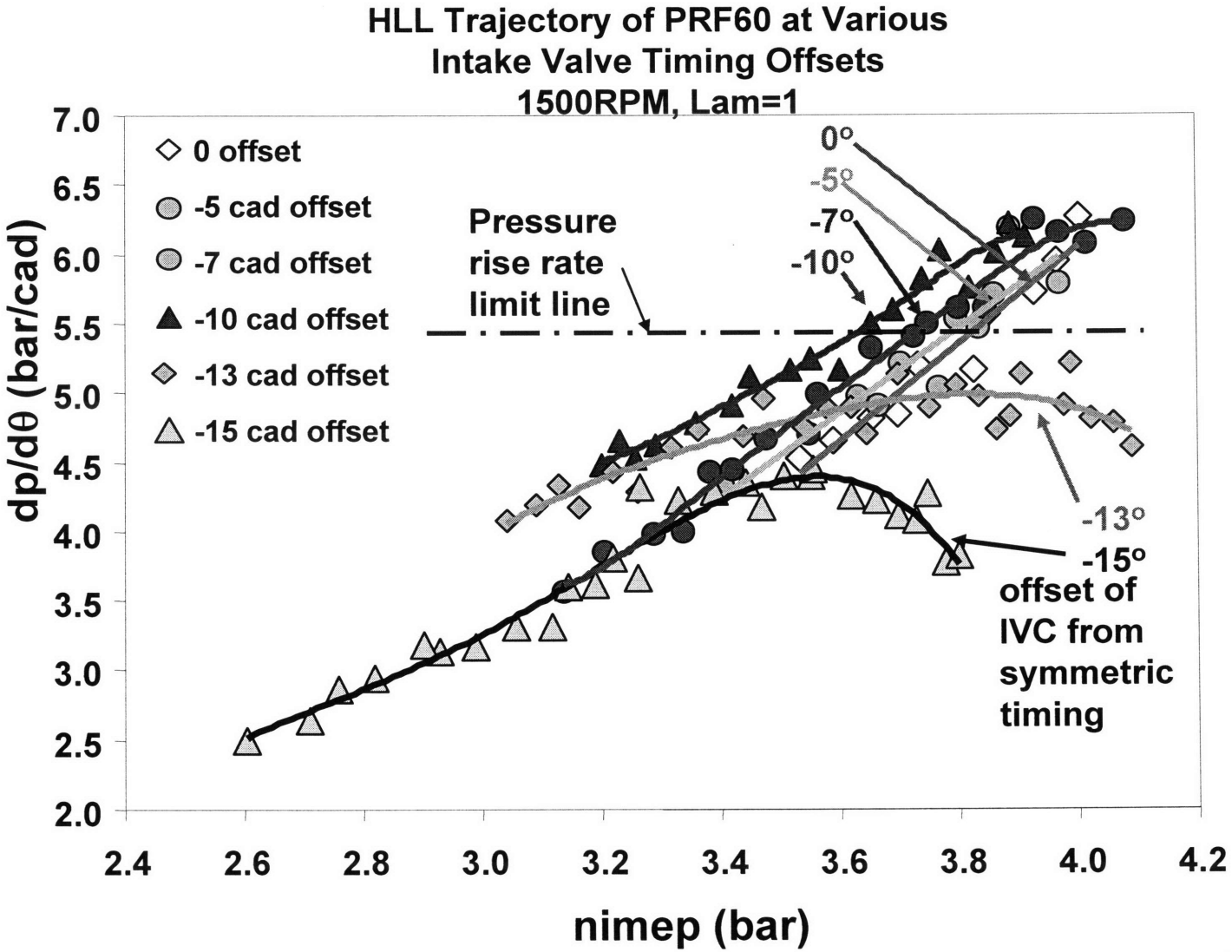

Figure 3.15: Effects of changing intake valve timing on PRF60 with lines of constant offset from symmetric at 1500 RPM

The same procedure was repeated for PRF90, except this time the offset was positive which means that the IVO was further away from TDC than EVC was at any given point. Figure 3.16 shows the relationship in the same fashion as with PRF60, but with a much greater variation in the data. As mentioned before PRF90 is very difficult to auto-ignite. This not only makes it hard to collect data, but also it makes that data less repeatable. The timings represented in Figure 3.16 are symmetric, +5 CAD, and +10 CAD offset, but do not behave in a similar fashion to what was shown with PRF60. The +5 CAD offset has the greatest pressure rise rate, where previous assumptions would lead one to believe that +10 CAD should have the greatest. Also, as the data was collected, it was observed that the combustion was not very stable at +10 CAD and it was very hard to get the engine to maintain combustion. It should be further noted that there are 3 runs of data taken at the symmetric operating condition, but do not correspond to each other with a great deal of accuracy, and neither do they coordinate well with previous values observed. This all casts a shadow of doubt over the validity of the data taken and thus those values presented in Figure 3.16 must be taken at face value. PRF90 is a very hard fuel to operate in this engine and data take far away from symmetric operating range comes with a great deal of variation and it makes it hard to find any sort of trends with the changing of intake valve timing.

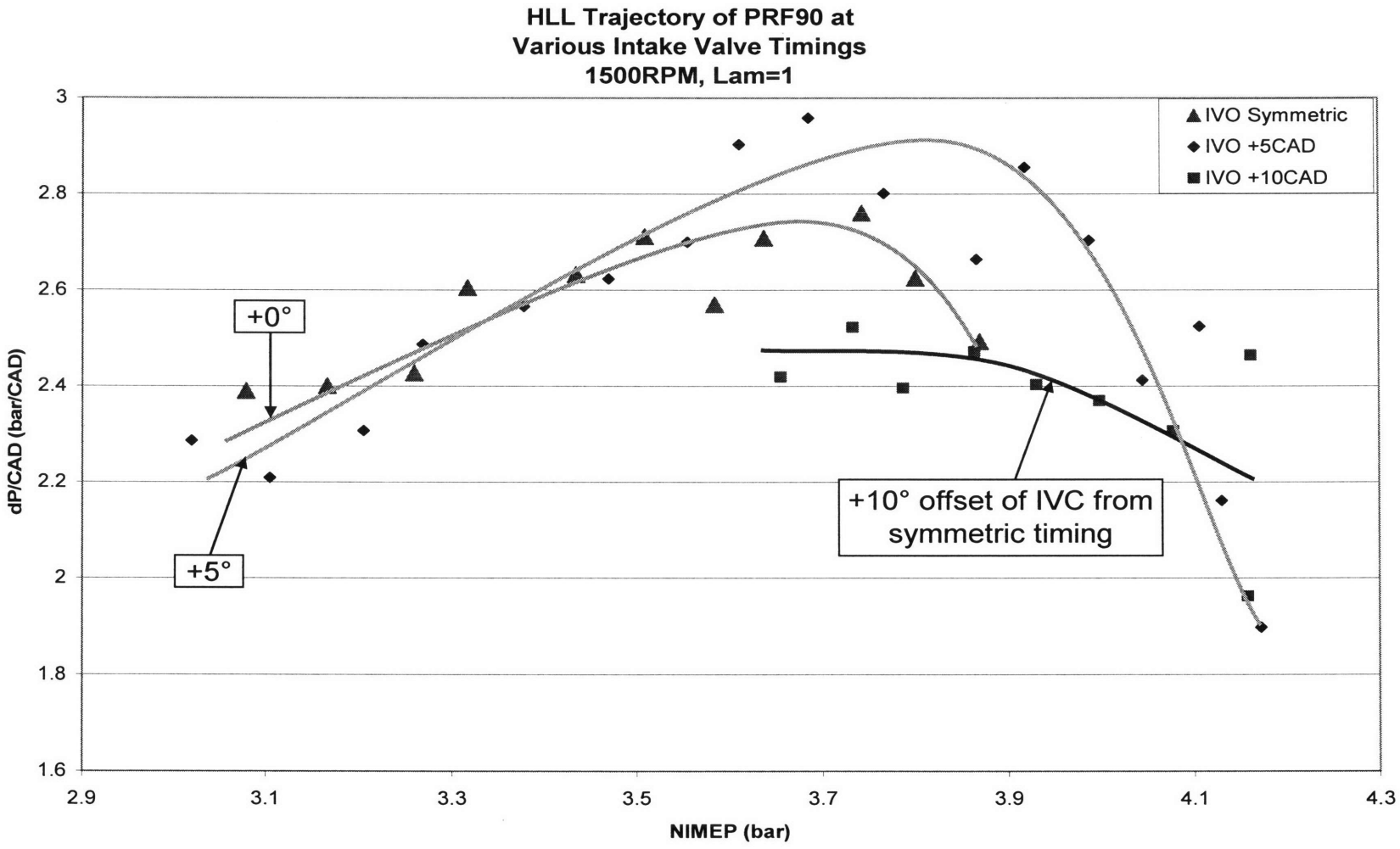

Figure 3.16: Effects of changing intake valve timing on PRF90 with lines of constant offset from symmetric at 1500 RPM

4 Conclusions

The high and low load limits of gasoline HCCI engine operating with NVO were assessed simulation and by engine experiments. The high load limit is severely constrained by NO_x emissions if a 3-way catalyst is not used. Maintaining a sufficient catalyst temperature constrains the low load limit. Engine experiments with PRF60, PRF90, and a extremely low aromatics and olefin gasoline showed that depending on the fuel the HLL could be pressure rise rate limited or ignition limited.

4.1 Simulation HLL:

The HLL in the simulations was constrained by a 0.13g NO_x/kg fuel which was derived from the EPA PZEV vehicle emissions standard. The effects of engine speed and boosting intake pressure were both analyzed. It was found that increasing the engine speed decreased the volumetric efficiency, and thus decreased the load that could be achieved at the NO_x limit. When the effects of boosted intake pressure were analyzed at constant engine speed it was found that increasing the intake pressure increased the load which could be achieved at that limit. While the HLL was found to be approximately 4.2 bar with significant turbo charging, a very high residual fraction (>70%) is required. These results make it seem that the operation of an HCCI engine without a catalyst is unlikely.

4.2 Simulation LLL:

A LLL was formulated based upon sustaining the catalyst temperature. Again, as with the HLL, both engine speed and boosted intake pressures were tested to see what effect they would have on the catalyst temperature. Since the catalyst temperature was maintained by the balance between the heat loss in the ambient and the exhaust enthalpy flow, the mass flow rate through the system determined the limit. This meant that at higher speeds the less load (therefore in-cylinder temperature) was necessary to maintain the temperature. Similarly, the greater boost enabled operation at lower in-cylinder temperature (and thus higher residual fraction). The lower value for LLL is achieved when the engine speed is the highest and the boosted intake pressure is the lowest. In the simulation this occurred at 3000 RPM and 1.0 bar intake pressure resulting in a NIMEP of ~1.5 bar. The one caveat is that the LLL usually occurs at idle conditions. In this case it is not desirable to have a high engine RPM because it uses more fuel, but with decreased engine speed also increases the load at the LLL, further decreasing the usable range of HCCI.

4.3 Experimental HLL:

Three fuels, PRF60, PRF90, and a blend denoted by Extremely Low Aromatics and Olefin were tested. The experiments were first done with symmetric valve timings; i.e. the IVO and EVC were at crank angles symmetric with respect to top dead center. Then a valve timing sweep was done. The HLL of the PRF90 fuel was limited by the misfire limit, and that of the PRF60 was pressure rise rate limited. The maximum pressure rise rate increased with increasing load for the pressure rise rate limit, and

decreased with increasing load for the misfire limit. However, for the ELAO blend, the load was not monotonic with respect to the pressure rise rate (dependency has the appear of a hook). In the end ELAO had the highest limit at ~3.95 bar, at which it was misfire limited, PRF90 was next with ~3.8bar, at which it was also misfire limited, and PRF60 was the lowest at 3.45 bar, at which it was pressure rise rate limited. These were all for 1500 RPM. Decreasing the engine speed did not affect which type of limit was reached, but it did affect the load at which it occurred. PRF60 increased to ~3.9 bar at 1000 RPM and PRF90 increased to ~4.05 bar at 1300RPM (ELAO was not tested at a lower speed).

To further investigate what was occurring with the types of limits PRF60 was tested at selected intake valve timing offsets. Non-monotonic dependency (the hooked curve) was observed with offsets of -13 and -15 CAD.

Overall these results provided a glimpse of the limitations and potentials for research forward. More research may be concentrated on the behavior at the limit and how the fuels approach the limit and try to connect them across speeds and fuel characteristics to see if an optimal blend or control strategy could be found.

5 Appendix: Fuel Calibration Curve

At the beginning of experimentation the fuel injectors were calibrated for future reference. The fueling pulse width was recorded during data collection, but was not used in calculations. Figure A.1 shows the correlation between the controlled fuel pulse width (ms) to the volumetric output of the injectors at 60psi of delivered fuel pressure. This with an approximate density of 750 kg/m^3[9] will provide the mass of fuel delivered to the cylinder per cycle.

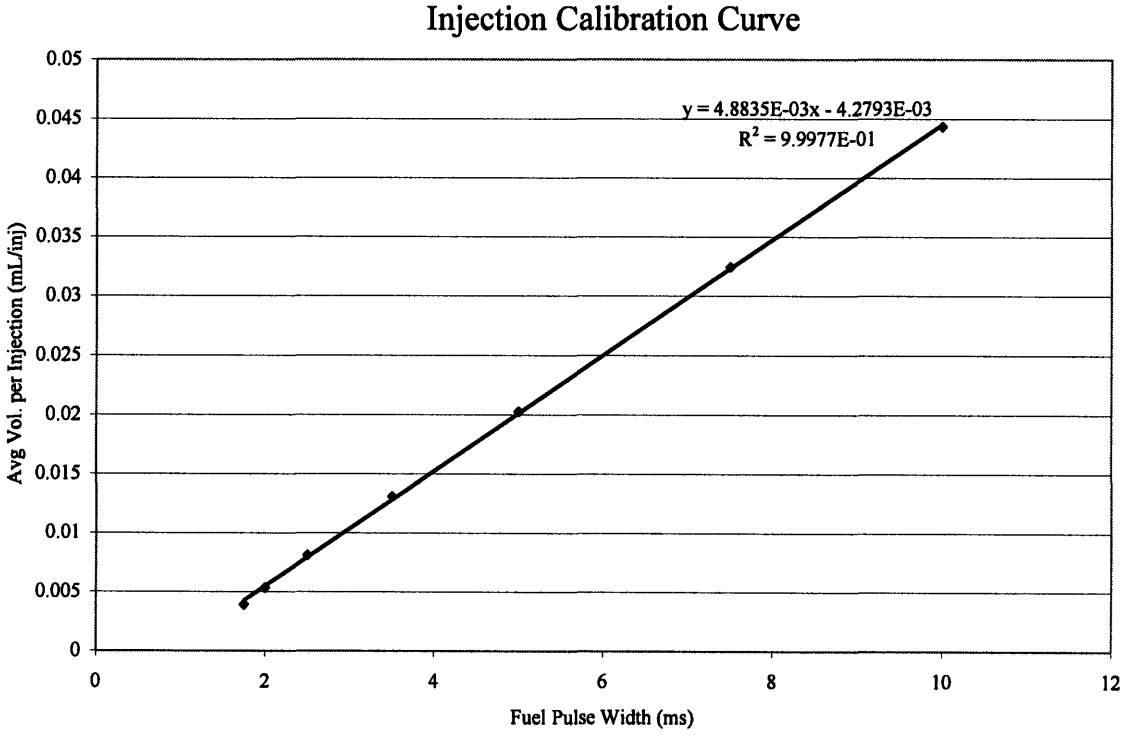

Figure 5.1: Injection Calibration Curve

References:

[1] Onishi, S., Jo, S.H., Shoda, K., Jo, P.D., Kato, S., "Active Thermo-Atmosphere Combustion (ATAC) – A New Combustion Process for Internal Combustion Engines", SAE 790501, 1979

[2] Najit, P.M., Foster, D.E., "Compression-Ignited Homogeneous Charge Combustion", SAE 830264, 1983

[3] Kontarakis, G., Collings, N., Ma, T., "Demonstration of HCCI Using a Single-Cylinder, Four Stroke Engine with Modified Valve Timing", SAE 2000-01-2870, 2000

[4] Kalghatgi, G., "Auto-Ignition Quality of Practical Fuels and Implications for Fuel Requirements of Future SI and HCCI Engines", SAE 2005-01-0239, 2005

[5] Shibata, G., Urushiara, T., "The Interaction between Fuel Chemicals and HCCI Combustion Under Heated Intake Air Conditions", SAE 2006-01-0207, 2006

[6] Yao, M., Zheng, Z., Zhang, B., Zheng, C., "The Effect of PRF Fuel Octane Number on HCCI Operation", SAE 2004-01-2992, 2004

[7] Andrea, M., "Effect of Ambient Conditions and Fuel Properties on Homogeneous Charge Compression Ignition Engine Operation", Doctoral Thesis, Massachusetts Institute of Technology, 2006

[8] Ricardo WAVE Software

[9] Heywood, J., "Internal Combustion Engine Fundamentals", McGraw-Hill, 1988

[10] Turns, S., "An Introduction to Combustion, Concepts and Applications", McGraw-Hill, 2000

[11] Angelos, J., "FUEL EFFECTS IN HOMOGENEOUS CHARGE COMPRESSION IGNITION (HCCI) ENGINES", Doctoral Thesis, Massachusetts Institute of Technology, 2008

[12] National Instruments LabVIEW Software